

Distributed/Cluster Computing for Data Stream Mining: Draft Notes

A thesis
submitted in partial fulfilment
of the requirements for the Degree
of
Master of Science
at the
University of Waikato
by
Vladimir Petko

University of Waikato
2016

Abstract

The thesis is focused on elucidating GPU computing feasibility for clustering tasks

Acknowledgements

Contents

Abstract	i
Acknowledgements	iii
1 General Purpose GPU Computing	2
1.1 Introduction	2
1.2 GPU Architecture	3
1.3 General Purpose GPU Computing Frameworks	5
1.3.1 High Level Languages	5
1.3.2 GPU-specific Languages	6
1.3.3 Low-Level Languages	7
1.3.4 Limitations	7
1.4 OpenCL 2.0	8
1.5 HSA Platform	9
1.5.1 HSA Queues	9
1.5.2 HSA Signals	10
1.5.3 HSA Memory Model	10
1.5.4 Implementation Notes	11
1.6 Conclusion	11
2 System Architecture	13
2.1 MOA interface	13
2.2 GPU Memory Limits	15
2.3 HSA Backend	15
2.4 OpenCL 2.0 features	15
2.5 Conclusion	16
3 k-Nearest Neighbours	17
3.1 Introduction	17
3.2 Exhaustive Search	18
3.2.1 Distance Calculation	19
3.2.2 Selection	19
3.2.3 Conclusion	20

3.3	Exact Clustering Methods	21
3.3.1	k-d Tree	21
3.3.2	Random Projection Trees	23
3.3.3	Random Projection	26
3.3.4	Random Projection Tree Search	28
3.4	Approximate Clustering Methods	28
3.4.1	Locality Sensivity Hashing	29
4	Stochastic Gradient Descent	34
4.1	Introduction	34
4.2	Approaches for SGD parallelisation	34
4.3	Hogwild!	36
4.3.1	Best Ball Optimization	36
4.3.2	Backoff scheme	36
4.4	1bit SGD	36
4.5	Stochastic Gradient Descent using OpenCL/HSA architecture	37
4.6	Conclusion	38
5	Experimental Results	40
5.1	Experiment Setup	40
5.2	Experiment Data	40
5.3	Evaluation	41
5.4	k-Nearest Neighbours	41
5.4.1	Exhaustive Search	41
5.4.2	k-d Tree	42
5.4.3	Random Projection Tree	43
5.4.4	Z-Order Search	45
5.5	Stochastic Gradient Descent	45
6	Conclusions and Future Work	48
6.1	HSA	48

List of Figures

1.1	CPU versus GPU hardware architecture. Reproduced from NVIDIA GPU ARCHITECTURE and CUDA PROGRAMMING ENVIRONMENT by Alan Tatourian[79]	3
1.2	GPU Memory Tiers. Reproduced from NVIDIA GPU ARCHITECTURE and CUDA PROGRAMMING ENVIRONMENT by Alan Tatourian[79]	4
1.3	GP GPU technologies tree. Reproduced from C. Nugteren, Improving the Programmability of GPU Architecture, p. 21 [62]	6
1.4	Kernel launch time on integrated Radeon R7 GPU(μ sec). . . .	8
2.1	SGD classifier training activity.	14
3.1	Interleaved distance calculation and sorting phases	18
3.2	Left; Four matrix-vector multiplication kernels designed to perform well at different shapes $m \times n$ of the matrix. Middle; Tuning mesh. Right; Best kernel in practice. The dashed line indicates the minimum 21504 rows needed in the matrix for full occupancy of the Nvidia Tesla C2050 card in a one-thread-per-row kernel. Note the logarithmic axes. Reproduced from High-Performance Matrix-Vector Multiplication on the GPU by Hans Henrik Brandenborg Sørensen[76]	19
3.3	Selection Algorithm Performance for $K=128$. Test configuration GPU R9 390, CPU AMD A8-7600, AMD Catalyst version 15.20.	20
3.4	k-d tree construction and NN-search pseudocode	22

3.5	Distributions with low intrinsic dimension. The purple areas in these figures indicate regions in which the density of the data is significant, while the complementary white areas indicate areas where data density is very low. The left figure depicts data concentrated near a one-dimensional manifold. The ellipses represent mean+PCA approximations to subsets of the data. Our goal is to partition data into small diameter regions so that the data in each region is well-approximated by its mean+PCA. The right figure depicts a situation where the dimension of the data is variable. Some of the data lies close to a one-dimensional manifold, some of the data spans two dimensions, and some of the data (represented by the red dot) is concentrated around a single point (a zero-dimensional manifold). Reproduced from Learning the structure of manifolds using random projections by Freund Yoav et al.[44]	23
3.6	Left: Partitioning produced by k-d tree. Right: Partitioning produced by Random Projection Tree. Reproduced from Learning the structure of manifolds using random projections by Freund Yoav et al.[44]	24
3.7	Random Projection Tree Pseudocode - Random Tree Max [37]	24
3.8	Random Projection Tree Pseudocode - Random Projection Tree Median Split[37]	25
3.9	Random projection tree median split node types	26
(a)	Small node, the maximum diameter is less than the mean diameter multiplied by the constant	26
(b)	Large node, the maximum diameter exceeds mean diameter multiplied by the constant	26

3.10	Fast Johnson-Lindenstrauss transform[24] vs. sparse matrix implementation[22] using ViennaCL. Test configuration GPU R9 390, CPU AMD A8-7600, AMD Catalyst version 15.20. The matrix multiplication test was aborted due to the out of memory error.	29
3.11	Z-Order Curve. Red lines highlight some region jumps. Green shows locality-preserving region.	31
4.1	Hogwild!-based stochastic gradient descent	39
5.1	Latency of k-NN exhaustive search on Infinimnist stream . . .	42
5.2	Accuracy of k-NN exhaustive search on Infinimnist stream . .	43
5.3	<i>TODO</i> Accuracy of k-NN exhaustive search on synthetic stream using constant size window (8192) and variable number of attributes	44
5.4	<i>TODO</i> Difference in accuracy of k-NN exhaustive search on synthetic stream using constant size window (8192) and variable number of attributes	44
5.5	<i>TODO</i> Query latency of k-NN exhaustive search on synthetic stream using constant size window (8192) and variable number of attributes	45
5.6	<i>TODO</i> exhaustive k-NN on Twitter stream	45
5.7	<i>TODO</i> k-d Tree Training on Infinimnist Stream	46
5.8	<i>TODO</i> k-d Tree query evaluation on Infinimnist Stream	46
5.9	<i>TODO</i> k-d Tree query evaluation on Twitter Stream	47
5.10	<i>TODO</i> Random Projection tree training on Infinimnist data .	47
5.11	<i>TODO</i> Random Projection tree test on Infinimnist data	47
5.12	<i>TODO</i> Random Projection tree training on Twitter data . . .	47
5.13	<i>TODO</i> Random Projection tree test on Twitter data	47
5.14	Iterative Z-Order query performance on RandomRBFGenerator data stream	47

List of Tables

Introduction

In real world applications such as industrial monitoring, sensor networks, financial data generate large unbounded streams of data which has to be processed with pre-defined response time. The processors capabilities limit the bandwidth of the stream which can be processed. Parallelizing processing algorithm will increase maximum bandwidth while maintaining the response time requirement.

Chapter 1

General Purpose GPU Computing

1.1 Introduction

The modern Graphical Processing Units (GPU) greatly outpace CPUs in arithmetic throughput and memory bandwidth for data-parallel tasks. Since 2001 the efforts were made to port data parallel algorithms to GPUs - first using shader languages such as HLSL, then with the release of Nvidia G80 in 2006 using extensions to the C programming language - CUDA[14]. Presently there is a number of programming frameworks targetting specifically GPU architecture such as CUDA[60], OpenCL[13], RenderScript[18], DirectCompute[6] and more generic parallel-processing frameworks such as OpenMP[16] and AMP[4] which provide GPU backend as one of the targets. The differences in the hardware architecture between CPU and GPU is reflected in the programming model of the traditional GPU-specific languages which contain hardware architecture specific language constructs. This chapter provides an overview of GPU architecture and most known programming frameworks, lists limitations of the traditional GP GPU programming. It also discusses the OpenCL 2.0 standard, which addresses some of the limitations and describes the Heterogenous System Architecture (HSA), an optimized platform architecture for

OpenCL 2.0.

1.2 GPU Architecture

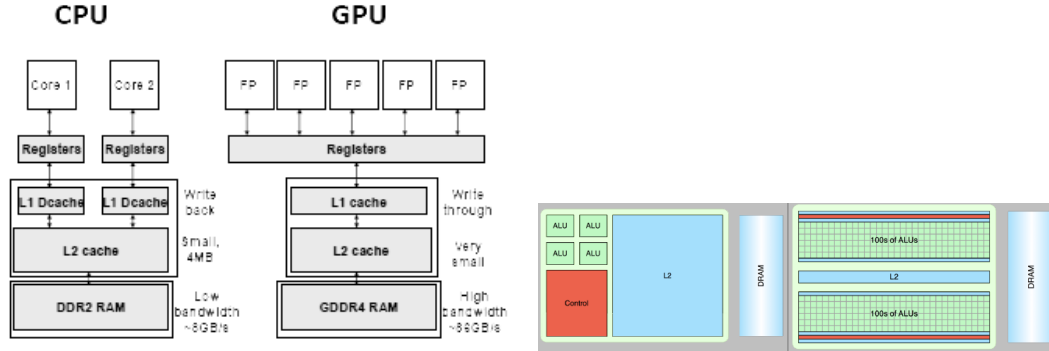


Figure 1.1: CPU versus GPU hardware architecture. Reproduced from NVIDIA GPU ARCHITECTURE and CUDA PROGRAMMING ENVIRONMENT by Alan Tatourian[79]

The main differences between modern CPU and GPU architectures are the level of parallelism and ability to directly address tiered memory. Modern CPU with 2 hex-cores support a maximum of 12 threads (24 with hyper-threading), where the minimal unit of execution for the NVIDIA GPU (called *wavefront*) is 32 threads. Modern GPUs implement a SIMT (Single Instruction - Multiple Thread) execution model (AMD/NVIDIA desktop GPUs) first introduced by NVIDIA in the G80 model[14]. The single unit of scalar instructions called *kernel* is scheduled to execute in blocks of data-parallel threads on SIMT hardware. Each instruction in a block is executed in a lock-step. The control divergence is emulated by *masking* - the device executes instructions from both branches of the conditional statement[19][60]. The CPU thread is a heavy-weight entity which is centered around execution of a specific task for an extended period of time. Whenever the CPU needs to preempt the running thread, its register state is stored and another thread takes over. This makes a context switch a costly operation and operating systems attempt to minimize number of context switches per second. The GPU context switch is an extremely lightweight operation and is routinely used for the latency-hiding -

whenever the wavefront is waiting on data, the GPU schedules another wavefront for execution. The GPU registers are private for each thread and are not reallocated until thread execution completes.

Modern CPUs provide a flat view of the operating system memory while GPUs divide memory in tiers based on the access speed:

- *private/register* - private to the current thread
- *local* - shared within a *threadblock*
- *global* - accessible by every thread

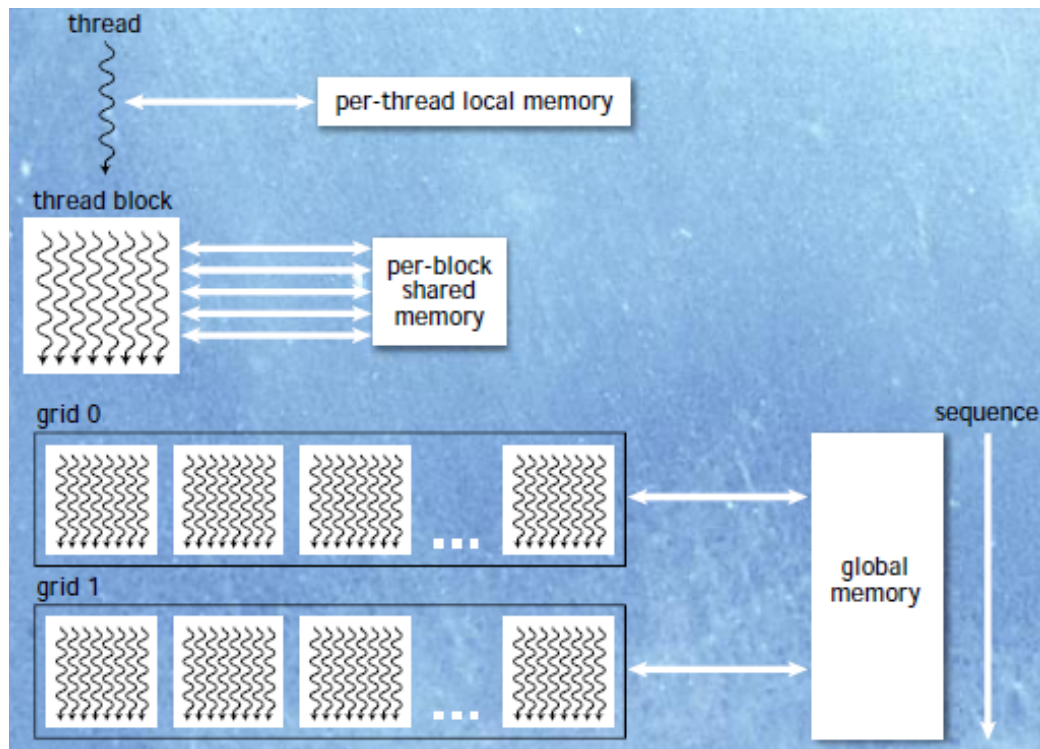


Figure 1.2: GPU Memory Tiers. Reproduced from NVIDIA GPU ARCHITECTURE and CUDA PROGRAMMING ENVIRONMENT by Alan Tatourian[79]

GPU programming uses the following abstractions:

- *Kernel* - a unit of execution
- *Thread* - a single unit of processed data
- *Threadblock* - a group of *threads* sharing the same *kernel* and *local* memory.

The unit of scheduling is called *wavefront* in AMD terminology or *warp* in NVIDIA and typically consists of 32 threads on NVIDIA and 64 on AMD hardware. The GPU chip is equipped with a number of SIMT cores which execute the same instruction for each *warp*. Divergence of control results in underload of the processing units and reduces performance. The branching should be reduced to wavefront granularity to avoid wasting execution cycles[75][60]. It should be noted that the wavefront size is a hardware specific feature and its optimization should be performed at the run-time.

1.3 General Purpose GPU Computing Frameworks

Existing General Purpose GPU (GP GPU) computing frameworks can be classified by the level of provided hardware abstraction: high-level frameworks integrate with existing high-level programming language such as Java to provide parallel computing capabilities without exposing any hardware details[15]. Traditional GPU languages such as CUDA[60] expose task scheduling and memory management giving the expert user fine-tuning capabilities. Low level languages provide an intermediate binary format compatible with multiple hardware targets. The tree of the GP-GPU technologies is presented in the Figure 1.

1.3.1 High Level Languages

OpenACC and OpenMP are high level parallel programming frameworks that specify a set of annotations, environment variables and library routines for shared memory parallelism in C/C++ and Fortran programs[1][16]. Microsoft C++ AMP[4] is a C++ library which enables parallel computations for CPU and GPUs (using Microsoft DirectX Shading Language). The Rootbeer GPU compiler provides for transparent compilation of Java code into CUDA[67]. Aparapi provides a way to generate OpenCL kernel code from Java, theoret-

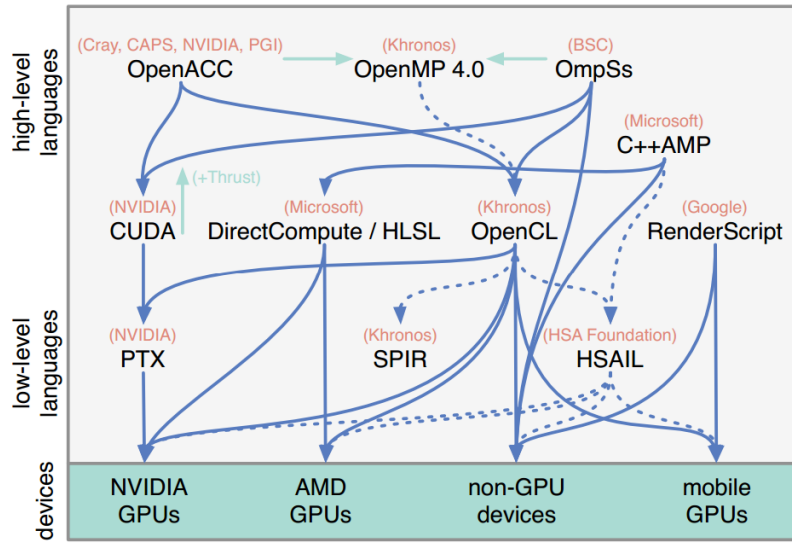


Figure 1.3: GP GPU technologies tree. Reproduced from C. Nugteren, Improving the Programmability of GPU Architecture, p. 21 [62]

ically allowing code which can be executed on CPU and offloaded to GPU if needed[2]. Project Sumatra is a OpenJDK project which focuses on the development of Hotspot virtual machine extensions capable of offloading JDK 8 Stream API[12] computations to the GPU[15].

1.3.2 GPU-specific Languages

GPU-specific languages provide a programming model consistent with the GPU hardware implementation.

- CUDA - A programming language for NVIDIA hardware based on the C language. Kernels are expressed as C-functions for one thread with parallelism defined at run-time by specifying dimensions of the execution grid and the thread blocks[60]
- OpenCL 1.X builds upon ideas implemented in CUDA by adding device management APIs and providing hardware-agnostic programming specification. OpenCL gives a *write once-run anywhere* guarantee but does not give any performance consistency guarantees across different hardware[77].

- **RenderScript** - an Android GPU computing component which uses OpenCL with Java binding programming model - C-style kernels and Java-based control code. RenderScript does not provide any APIs for the *workgroup* size control in a bid to provide performance portability between different devices[18].
- **DirectCompute/HLSL** - Microsoft extension to Direct3D API for general purpose computing. It uses proprietary scripting language first introduced in DirectX 9 that has a limited support for double precision computing. DirectCompute only allows to specify the *workgroup* size at the compile time[6].

1.3.3 Low-Level Languages

The low level assembly representation is used to abstract compiler implementation from the actual hardware since each model or even revision may have a different instruction set. The translation is performed by a *Just-In-Time* compiler before the kernel execution. Each vendor provides different low level specifications: NVIDIA CUDA uses Parallel Thread Execution and Instruction Set Architecture (PTX ISA)[17], Khronos Group specifies Standard Portable Intermediate Representation(SPIR)[20], and HSA Foundation specifies Heterogenous System Architecture Intermediate Language (HSAIL)[21].

1.3.4 Limitations

Input Size The massively parallel nature of GPU platforms require a certain amount of data to be passed to the kernel to achieve maximum performance. Figure 1.4 shows execution time of a kernel which assigns index to each array element $X_i = i$ on AMD A8-7600 integrated GPU. The execution time starts to increase when input size is above 1024 and remains constant for lower values. To maximum performance on the integrated GPU of AMD A8-7600 will be achieved when input size will exceed 1024 elements.

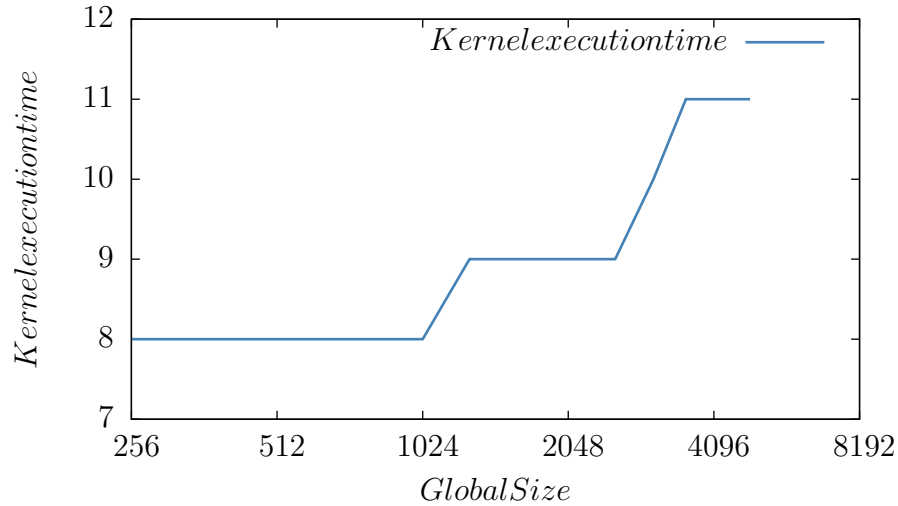


Figure 1.4: Kernel launch time on integrated Radeon R7 GPU(μ sec).

GPU Memory Size and Host-GPU Transfer The discrete GPU requires transfer of data from the host to the GPU memory which adds additional overhead to the computations and requires task partitioning according to the memory specification of the GPU[74]. Memory transfer is a bottleneck for Aparapi and its developers allow explicit memory management[2]. This effectively reduces a framework which promises general CPU-GPU interoperability to a mere Java wrapper of the OpenCL API.

Kernel Launch Constant time is needed to setup kernel launch which might offset any gain from parallelization if the data can be processed faster sequentially. Some algorithms have stop conditions that have to be checked to find out if the algorithm requires additional iterations. OpenCL 1.X specification does not allow scheduling of the kernel execution from within the kernel itself. In this case we need to synchronize with the host portion of the program to set up additional kernel launches introducing a bottleneck.

1.4 OpenCL 2.0

OpenCL 2.0 standard[13] introduces several features which attempt to address limitations of GPU programming:

- Shared Virtual Memory - both host and kernel code share the same address space thus either hiding memory transfers (discrete GPU driver stack) or if backed by the hardware architecture such as HSA eliminate the need for it[21].
- Dynamic Parallelism - OpenCL 2.0 allows scheduling of kernels from within a kernel without host interaction reducing the host CPU-GPU synchronization bottleneck.
- Pipes - the pipes feature allows for passing data from kernel to kernel without processing the whole input.

1.5 HSA Platform

AMD introduced the Heterogeneous System Architecture platform as an optimized platform architecture for OpenCL 2.0. Its specification introduces a set of requirements that allow both GPUs and CPU share the same memory space, synchronize execution using signals and atomics, and to schedule execution both from the GPU and the CPU[21]. Task execution is performed by *agents* which represent CPU or GPU nodes. The task execution is scheduled via *queues* and synchronized using *signals*. HSA memory model guarantees sequential consistency for the correctly synchronized programs. At the moment (Feb 2016) there is a OpenCL 2.0 - HSAIL compiler available[10] and a Linux-based runtime environment[9].

1.5.1 HSA Queues

HSA uses queues to schedule code execution. A HSA *queue* is a ringbuffer which contains *packets* with either call or synchronization parameters. The queue maintains two indexes - read index and write index. Write index is modified by the user and used to submit packets to the queue. The read index is updated by the packet processor whenever the packet is taken for

execution. As soon as a packet is written to the queue, the ownership is taken by the HSA packet processor and it may change packet contents at any time[21]. Compared to traditional dispatch where the execution is scheduled via user-mode and kernel-mode driver layers, the HSA dispatch intends to be lightweight and a source-agnostic way of scheduling execution. The HSA Queues support work-stealing, that is several HSA agents may be attached to the queue to share the workload.

1.5.2 HSA Signals

HSA uses *signals* to perform synchronization between the host and kernels being executed or to signal completion of the task. A *signal* is essentially a shared memory variable modified by the HSA agent. The runtime environment provides a way to check the value of the signal or wait for the specific value.

1.5.3 HSA Memory Model

Sequential consistency was first defined by L. Lamport as “..the result of any execution is the same as if the operations of all the processors were executed in some sequential order, and the operations of each individual processor appear in this sequence in the order specified by its program.” Modern processors (ARM, x86, Itanium, POWER) introduce a relaxed memory model to allow a range of hardware optimizations to provide better performance by reordering load and store operations[56]. The HSA platform specification states[21]

The HSA memory consistency model is a relaxed model based around RCsc semantics on a set of synchronizing operations. The standard RCsc model is extended to include fences and relaxed atomic operations. In addition HSA includes concepts of memory segments and scopes.

Similar to Java Memory Model[55] it guarantees sequential consistency for correctly synchronized programs, that is ‘synchronizing operations meet the requirements for sequential consistency within each scope/segment instance’[21]. This specification introduces several memory segments:

- Global segment, shared between all agents.

- Group segment, shared between work-items in the same work-group in a HSAIL kernel dispatch.
- Private, private to a single work-item in a HSAIL kernel dispatch.
- Kernarg, read-only memory visible to all work-items in a HSAIL kernel dispatch.
- Readonly, read-only memory visible to all agents

Each particular memory location is always associated with one and only one segment and all operations apply to only one segment with the exception of fence operations[21]. In addition to memory segments the HSA memory model introduces *scopes* : wavefront, work-group, component and system. They can be used to reduce visibility of the memory operation compared to the default supported by the segment. The global segment may use any of the specified scopes, group segments are limited to wavefront and workgroup scopes [21]. Different workgroups accessing a global variable within the same workgroup scope will work with different instances of the variable. Write serialization only applies to the operations within the segment/scope that they specify.

1.5.4 Implementation Notes

At the time of writing (February 2016) the HSA Runtime implementation ignores sequential barrier flag thus iterative algorithms have to explicitly synchronize kernel execution using signals to avoid starting a new kernel before the previous finishes. There is a constant time needed to setup kernel launch, e.g. for AMD A8-7600, it is 6 μ sec using HSA.

1.6 Conclusion

Modern specifications, such as OpenCL 2.0 and HSA, attempt to address some of the latency issues of GPU programming by the introduction of shared memory and lightweight dispatch/data passing mechanisms. This work will focus

on the evaluation of suitability of those technologies for the latency-sensitive processing of the data streams.

Chapter 2

System Architecture

We have implemented a data stream processing library which provides a set of classification algorithms for Massively Online Analysis(MOA)[31]. This library uses existing linear algebra package ViennaCL[80] which allows multiple backends such as CUDA, OpenCL, CPU. We have built some machine learning algorithms such as nearest neighbours search and stochastic gradient descent using its interfaces.

2.1 MOA interface

The ViennaCL library is implemented in C++ and as such requires Java Native Interface[11] to be used to interface from the Java Virtual Machine. Java Virtual Machine manages its own memory space and garbage collection may move data at any time. JNI provides two mechanisms to access array data from native code. First is copying - a java pointer is locked by a critical section and array content is copied to the native array. Second one skips the copying and provides direct access to the java pointer. Both involve entering and exiting a critical section and impose significant performance loss due to the copying and locking overhead. Those costs can not be avoided but can be minimized by moving them to the instance creation/modification time - the object constructor will call the native method which allocates the native data structures and moves data from the Java storage to the native one.

The alternative solution uses the *java.misc.Unsafe* class to manipulate offheap memory directly. The native code allocates GPU shared virtual memory and passes the pointer to the Java implementation. Java code uses *java.misc.Unsafe* methods to update data in parallel to training. Figure 2.1 shows the training process of the Stochastic Gradient Descent classifier. The instances are accumulated in batches on the main thread of execution, the batches are passed to the data transfer thread that handles CPU-GPU transfer and then the training thread is triggered to run GPU kernels. Whenever the evaluation (*getVotesForInstance*) is called, the threads process the last available batch and meet at the synchronization point, stopping execution.

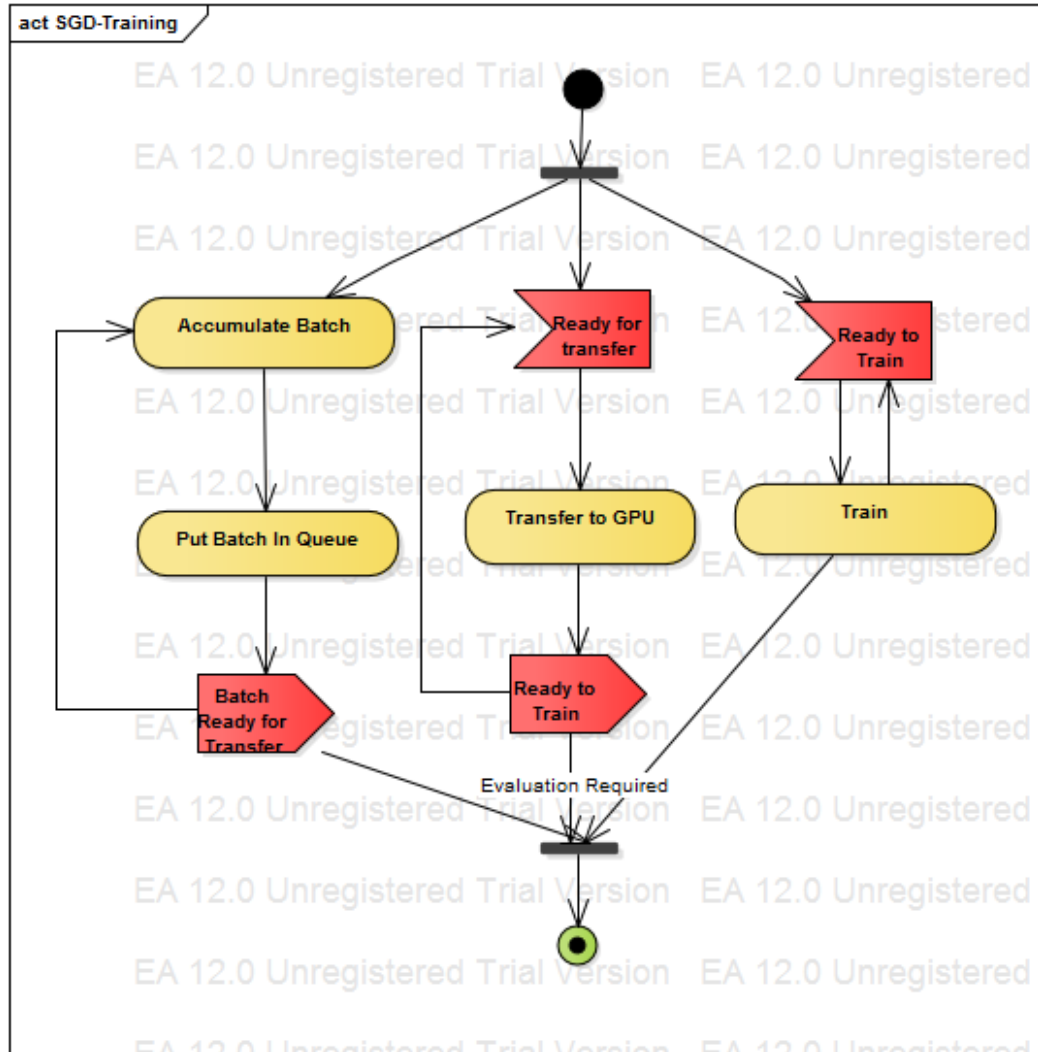


Figure 2.1: SGD classifier training activity.

2.2 GPU Memory Limits

The library implementation stores the instance data as the native ViennaCL types. This implies that for GPU ViennaCL backends the data will be stored in GPU memory that may be insufficient for larger problems. In such case partitioning will be used - the problem data is kept in the Java memory as a collection of *weka.core.Instance* objects and offloaded to GPU-backed context on as needed basis. The *weka.core.Instance* class represents the attribute values as a vector of double precision numbers. Modern consumer GPUs provide far better floating point performance than double performance. For instance modern AMD GPUs have 8x scale that is floating point performance is 8x better than double one (R390, R290). NVIDIA GPUs have 32x scale(Maxwell)[8]. There are several works that explore using fixed precision numbers to reduce memory requirements of machine learning tasks[69][49]. An alternative precision implementation will impose the overhead costs of double to fixed/floating point conversion, if a GPU classifier will be used, for instance, as a part of the meta-classifier ensemble.

2.3 HSA Backend

This work adds a new HSA backend to the ViennaCL library based on the HSA Runtime[21]. This implementation is tuned for Kaveri AMD APU and uses the same set of OpenCL kernels as the OpenCL backend. In the HSA backend the main system memory is transparently mapped to GPU memory and vice-versa, allowing to use vector or matrix element-addressing operations without first copying data to the CPU memory space.

2.4 OpenCL 2.0 features

At the time of writing (February 2016) the OpenCL 2.0 features such as work-group functions and device enqueue impose significant performance impact.

The library uses Shared Virtual Memory buffers to facilitate easy switching between OpenCL and HSA backends. The ViennaCL types are constructed from *cl_mem* representation of the shared virtual memory buffers.

2.5 Conclusion

The library provided as a part of this work is heterogenous. It uses a Java platform at the top level to interface with MOA and perform high-level computation. The linear algebra primitives and GPU interface are implemented in C++ and interface with the Java part via Java Native Interface. To reduce the overhead of Java to native code data transfers, this implementation uses *sun.misc.Unsafe* that might be incompatible with the future Java releases. The library does not use OpenCL 2.0 features as tests show that they provide a negative performance impact at the time of writing. The training interface uses a latency-hiding trick to maximize GPU load for the model training. The test interface *getVotesForInstance* performs synchronously and strives to provide the result with the lowest possible latency.

Chapter 3

k-Nearest Neighbours

3.1 Introduction

The k-Nearest Neighbours method[36] is a non-parametric method used for classification and regression. It computes a given instance distance to the examples with known labels and either provides a class membership for the classification which is a class most common among nearest neighbours or an object property value which is an average of the nearest neighbours. The error rate is bounded by twice the Bayes error if the number of examples approaches infinity[36]. Online implementation of the algorithm uses a sliding window of example instances updated by the data stream. Window size, instance dimensionality and allowed error bounds define the optimal approach to solving the k-Nearest Neighbours problem. *Exhaustive Search* has high computational complexity for the queries, but provides a constant update time. *Exact Clustering Methods* partition the search space to achieve logarithmic query complexity at the expense of the window update time. *Approximate Clustering Methods* reduce search space dimensionality to provide an approximate result with a given error bound. GP GPU computing may be used to accelerate their runtime though success for discrete GPUs depends on developer ability to eliminate branching, optimize memory access, and avoid excessive Host-GPU transfers. The latter poses a most significant problem for online

k-Nearest neighbours implementations. This chapter reviews the *Exhaustive Search*, some of the *Exact Clustering Methods* and *Approximate Clustering Methods* and provides notes on GP GPU implementation.

3.2 Exhaustive Search

The exhaustive approach to Nearest Neighbour search is to compute distance to each instance present in the sliding window. The computational complexity of the query $O(Nd)$ where N - number of instances and d - number of attributes. The GP GPU implementation of the exhaustive search consists of distance calculation and selection phase. The distances to the query can be computed using standard vector and matrix routines provided by GP GPU libraries implementing Basic Linear Algebra Subroutines(BLAS)[7][5][80]. The selection phase finds the nearest examples to the query out of all the computed distances. Sismanis et. al[74] provide time complexity of reduced sort algorithms, evaluate their performance on GPU and propose to interleave distance calculation and selection phases to hide latency as shown in Figure 3.1. This approach allows to obtain better performance on low window sizes[59].

The data for the distance calculation should be offloaded to GPU, while it performs the selection phase. The sliding window is partitioned, if needed, across multiple GPUs according to the GPU memory capabilities and does not use instances spatial information.

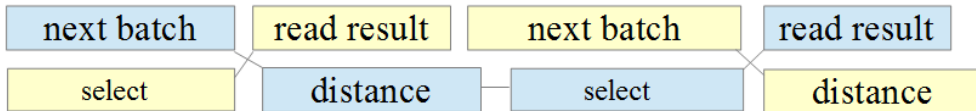


Figure 3.1: Interleaved distance calculation and sorting phases

3.2.1 Distance Calculation

The optimal implementation depends on the size of the window and number of attributes present[76]. For the small instance size (≤ 100) and windows of less than 10^4 elements one thread per instance implementation will provide the best solution. Best all around distance calculation should apply different strategies depending on the window size and number of attributes[76]. The alternatives are presented in the Figure 3.2.

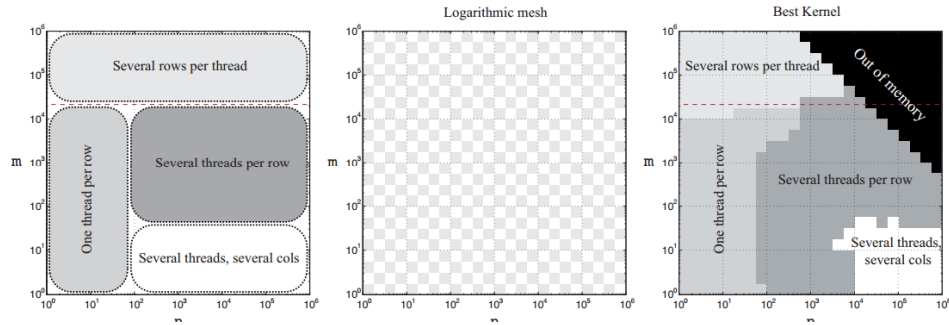


Figure 3.2: Left; Four matrix-vector multiplication kernels designed to perform well at different shapes $m \times n$ of the matrix. Middle; Tuning mesh. Right; Best kernel in practice. The dashed line indicates the minimum 21504 rows needed in the matrix for full occupancy of the Nvidia Tesla C2050 card in a one-thread-per-row kernel. Note the logarithmic axes. Reproduced from High-Performance Matrix-Vector Multiplication on the GPU by Hans Henrik Brandenborg Sørensen[76]

The distance calculation primitive provided as part of this master thesis uses one thread per row approach.

3.2.2 Selection

Alabi, et.al[25] evaluated different selection strategies based on bucket sort algorithm and Merrill-Grimshaw[57] implementation of radix sort.

Figure 3.3 shows performance of different selection strategies - merge sort from AMD Bolt library[3], bitonic sort similar to reference AMD implementation and radix select based on Alabi, et. al. implementation[25]. The CPU sort and choose is a clear winner for small window sizes, e.g. 4096 for the test hardware. The larger windows should be processed by radix select. The

threshold will be different for each CPU/GPU combination and should be tuned by the runtime.

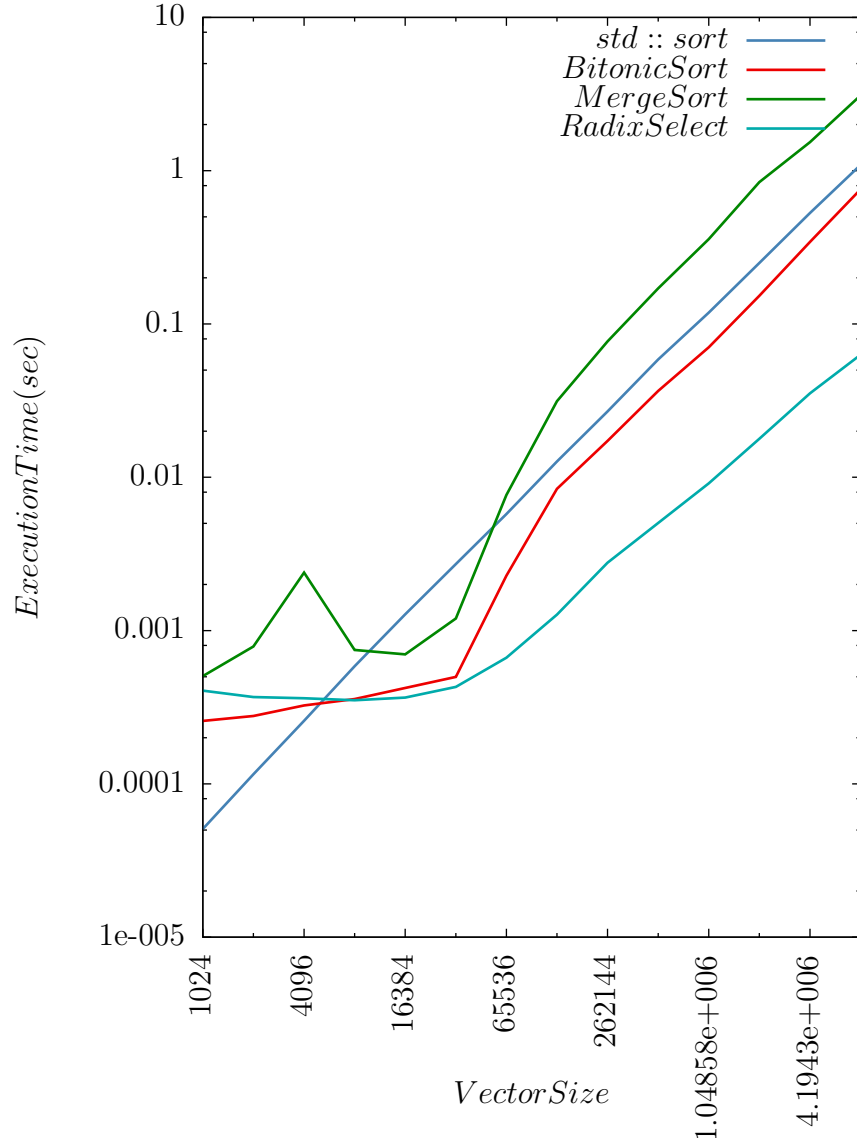


Figure 3.3: Selection Algorithm Performance for K=128. Test configuration GPU R9 390, CPU AMD A8-7600, AMD Catalyst version 15.20.

3.2.3 Conclusion

Exhaustive Search is a basic building block of the k-nearest neighbours algorithms. It is mandatory if we need to obtain an exact solution and is used to refine approximate methods results. The distance calculation parallelisation strategy should be adapted to the instance and windows size. Radix sort-based algorithm should be used for selection.

3.3 Exact Clustering Methods

Clustering techniques are widely used to limit the number of distance calculations needed for a nearest neighbour search. Space partitioning by vector dimensions is used by the k-d tree method[46], the random projection tree[44] provides a data structure splitting the search space along random vectors. Metric trees such as ball tree[63], cover tree[30], random ball cover[34] provide solutions for finding nearest neighbours in general metric space by organizing data points in groups around some centroids.

3.3.1 k-d Tree

The $k - d$ tree [46] is a balanced binary tree where each node represents a set of points $P \in \{p_1 \dots p_n\}$ and its children are disjoint and almost equal sized subsets of P . The tree is constructed top-down, the initial set of points is split along the widest dimension or using other criteria until the predefined number of points in child nodes is reached. The tree can be constructed in $O(n \log n)$ time and occupies linear space. Weber *etal*[81] have shown that $k - d$ tree is outperformed by the exact calculation at moderate dimensionality ($n > 10$) and results in full processing of the data points if the number of dimensions is large enough. It follows that the $k - d$ tree requires $N \gg 2^{(dimensions)}$ points to examine less points than exhaustive search.

The listing of the $k - d$ tree construction and nearest neighbours search pseudocode is shown in the Figure 3.4. Parallel $k - d$ tree construction on GPU utilizes breadth-first approach[82][72] - the $k - d$ tree is constructed top-down with the split criteria computed in parallel for all nodes at the specific level. The priority queue based nearest neighbours search using k-d trees as shown in Figure 3.4 does not benefit much from the GP GPU parallelism due to the branch divergence and irregular memory access patterns[48]. The $k - d$ tree search approach presented by Gieske et. al[48] focuses on parallel execution of nearest neighbour queries in a lazy fashion. The query points are accumulated

```

1  tree_node create_tree(pointList, level)
2  {
3      int dim = select_dim(pointList); // select split dimension according to
4      // pre-defined criteria, e.g. level mod total_dimensions
5      splitVal = select_split_value( pointList, dim); // select split value
6      // according to pre-defined criteria
7      // e.g. median value of point[dim]
8
9      left = {};
10     right = {}
11     for (point : pointList )
12     {
13         if (point[dim] > splitVal)
14             right += point;
15         else
16             left += point;
17     }
18     node = {
19         .location = splitVal,
20         .dim = dim,
21         .left = create_tree(left, level + 1),
22         .right = create_tree(right, level + 1)
23     };
24     return node;
25 }
26
27 void search(Heap nearest_neighbours, tree_node root, point p)
28 {
29     if (root.is_leaf())
30         nearest_neighbours.update(root);
31     else
32     {
33         split = root.location;
34         dim = root.dim;
35         if (p[dim] < split ) // search "closest" node
36             search(nearest_neighbours, root.left, p)
37         else
38             search(nearest_neighbours, root.right, p)
39
40         distance_to_split_plane = abs(split-p[dim]);
41         distance_to_point = abs(nearest_neighbours.furthest_point()[dim]-p[dim])
42         if (distance_to_point >=distance_to_split_plane) // outer radius of NN heap
43             intersects the split plane
44             {
45                 if (p[dim] < split )
46                     search(nearest_neighbours, root.right p)
47                 else
48                     search(nearest_neighbours, root.left, p)
49             }
50     }
51 }

```

Figure 3.4: k-d tree construction and NN-search pseudocode

in the leaf nodes of the kd-tree until enough of them are present and then they are processed as a batch. This solves the issue of GPU underutilization and low performance if leaf nodes are processed sequentially for each example. An other approach would be to compute distances to the leaf nodes split planes[82] to provide a short-list of the leaf nodes for k-nearest neighbours search.

3.3.2 Random Projection Trees

The $k - d$ tree provides an effective partitioning mechanism for low data dimensionality but suffers in higher dimensions[81]. Many machine learning problems that are expressed in high dimensional space have lower intrinsic dimension as shown in Figure 3.5. Random projection tree exploits this fact

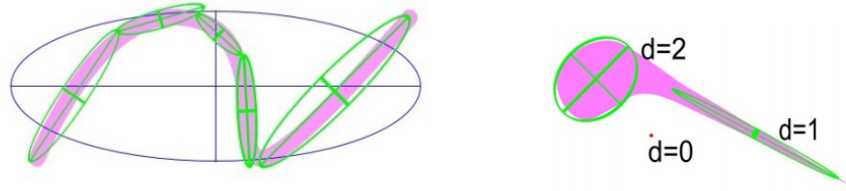


Figure 3.5: Distributions with low intrinsic dimension. The purple areas in these figures indicate regions in which the density of the data is significant, while the complementary white areas indicate areas where data density is very low. The left figure depicts data concentrated near a one-dimensional manifold. The ellipses represent mean+PCA approximations to subsets of the data. Our goal is to partition data into small diameter regions so that the data in each region is well-approximated by its mean+PCA. The right figure depicts a situation where the dimension of the data is variable. Some of the data lies close to a one-dimensional manifold, some of the data spans two dimensions, and some of the data (represented by the red dot) is concentrated around a single point (a zero-dimensional manifold). Reproduced from Learning the structure of manifolds using random projections by Freund Yoav et al.[44]

by splitting data along randomly chosen unit vectors as opposed to splitting along dimension axes in the k-d tree method as shown in Figure 3.6 [44]. The method performs a one dimensional random projection of the data points and splits them at the median of the projections.

The random projection tree split rules are presented in Figures 3.7 and 3.8. Figure 3.9 illustrates node selection for random projection tree median split

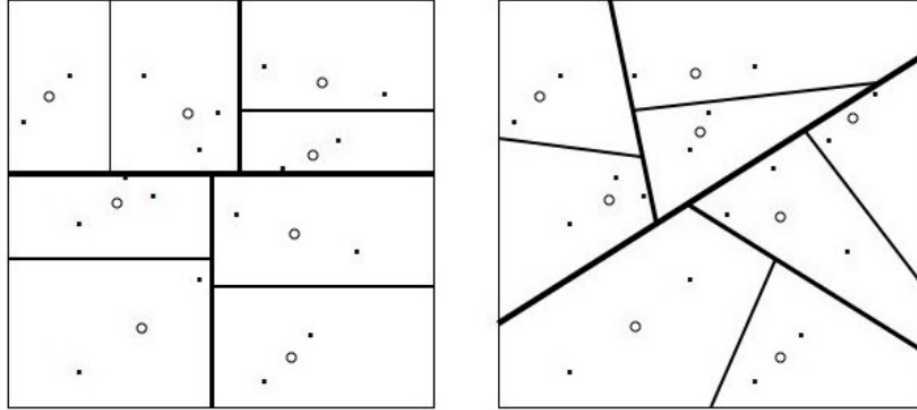


Figure 3.6: Left: Partitioning produced by k-d tree. Right: Partitioning produced by Random Projection Tree. Reproduced from Learning the structure of manifolds using random projections by Freund Yoav et al.[44]

```

1  tree_node random_tree_max(pointList, num_dimensions)
2  {
3      v = random_vector(num_dimensions);
4
5      x = pointList[ random() ];
6      y = max (distance( y in pointList, x) );
7      sigma = uniform_random(-1;1) * 6 * distance(x,y) / sqrt(num_dimensions);
8      split = median ( dot(v, x in pointList)+ sigma ) ;
9      left = {}
10     right = {}
11     for (x in pointList)
12     {
13         if (dot(v,x) <= split)
14             left += x;
15         else
16             right +=x;
17     }
18     node = {
19         .vector = v,
20         .split = split,
21         .left = create_tree(left, num_dimensions),
22         .right = create_tree(right, num_dimensions)
23     };
24     return node;
25 }

```

Figure 3.7: Random Projection Tree Pseudocode - Random Tree Max [37]

```

1  tree_node random_tree_mid(pointList, num_dimensions, c)
2  {
3      diameter = max( distance(x in pointList, y in pointList));
4      avg_diameter = mean(distance(x in pointList, y in pointList));
5      if ( diameter <= c* avg_diameter)
6      {
7          // small node, split using random projection threshold
8          v = random_vector(num_dimensions);
9          split = median( dot(x in pointList, v) );
10         left = {}
11         right = {}
12         for (x in pointList)
13         {
14             if (dot(v,x) <= split)
15                 left += x;
16             else
17                 right +=x;
18         }
19         node = {
20             .rule_type = dotproduct
21             .vector = v,
22             .split = split,
23             .left = create_tree(left, num_dimensions),
24             .right = create_tree(right, num_dimensions)
25         };
26         return node;
27     }
28     else
29     {
30         // large node. split by the distance from median
31         meanPoint = mean(x in pointList)
32         split = median( distance(x in pointList, meanPoint));
33         left = {}
34         right = {}
35         for (x in pointList)
36         {
37             if (distance(x, meanPoint) <= split)
38                 left += x;
39             else
40                 right +=x;
41         }
42         node = {
43             .rule_type = distance
44             .mean = meanPoint,
45             .split = split,
46             .left = create_tree(left, num_dimensions),
47             .right = create_tree(right, num_dimensions)
48         };
49         return node;
50     }
51 }
52 }
53 }

```

Figure 3.8: Random Projection Tree Pseudocode - Random Projection Tree Median Split[37]

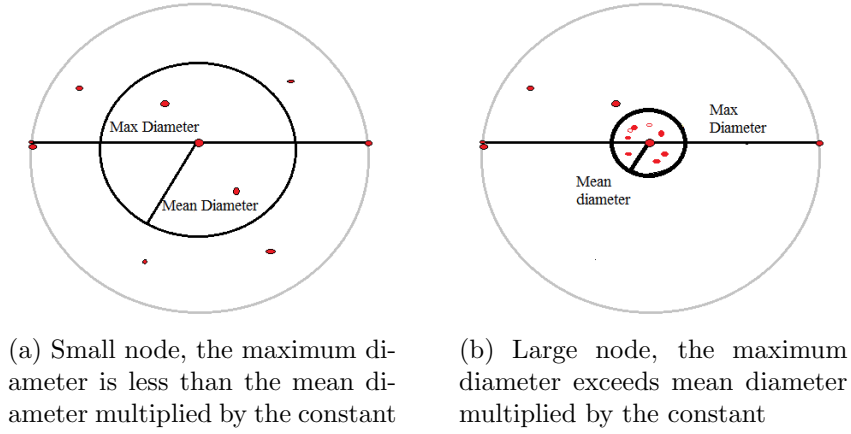


Figure 3.9: Random projection tree median split node types

rule.

The projections along then chosen random vectors may be computed in a batch as a matrix by vector multiplication. The computation of projections of high dimensional data for the split criteria can be also viewed as a random projection operation described by Johnson and Lindenstrauss[51] and be implemented more efficiently than naive approach.

3.3.3 Random Projection

The seminal paper by Johnson and Lindenstrauss[51] established that for euclidian spaces any $x \in \mathbb{R}^n$ can be embedded into \mathbb{R}^k with $k = O(\log n / \epsilon^2)$ by projecting x in \mathbb{R}^k using projection $k \times n$ matrix Φ without distorting inter-point distances by more than $(1 \pm \epsilon)$ and $k \geq O(\log n)$. Johnson and Lindenstrauss[51] has shown that Johnson-Lindenstrauss condition holds for matrices with the following properties:

- Spherical symmetry - For any orthogonal matrix $A \in O(d)$, Φ multiplied by A and Φ have the same distribution.
- Orthogonality - rows are orthogonal to each other
- Normality - the rows are unit-length vectors

The lower bound of k was refined in several papers[43][38][50][22] with Dasgupta and Gupta[38] proving it to be $k \geq 4(\epsilon^2/2 - \epsilon^3/3)^{-1} \ln(n)$ for $\epsilon \in (0, 1)$, where k - projection dimensionality, n - source dimensionality, ϵ - error. For high n this bound will still be too large to effectively employ low dimensionality search methods such as $k - d$ tree. An alternative would be to utilize very low dimensional space and then use disjunction to find the desired result. This approach is essentially an iterative random projection tree search where the dataset is split along leaf nodes.

The efficient implementation of the random projection-based algorithms requires a simple approach to construct Φ and a way to compute projection faster than naive multiplication of data point by $k \times n$ matrix. Achlioptas[22] achieved relatively sparse transformation matrix for random projection by proving that Johnson-Lindenstrauss condition holds if elements of the projection matrix are chosen independently according to the following distribution:

$$\begin{cases} +(n/3)^{-1/2}, P = 1/6 \\ 0, P = 2/3 \\ -(n/3)^{-1/2}, P = 1/6 \end{cases}$$

where n - source dimension and P - probability. This method provides a 3-fold speedup over the original one [51], since 2/3 of the transformation matrix elements are zero. Nir Ailon and Edo Liberty[24] have developed an almost optimal random projection transformation with runtime of $O(n \log n)$ as opposed to $O(kn)$ of the naive implementation. The main idea of the method is the application of the Heisenberg principle in its signal processing interpretation that both signal and its spectrum can not be both sharply localized. Thus applying Fourier transform to the sparse input vector will increase its support and will allow to make the transformation matrix even more sparse. To prevent the opposite, sparsification of the dense vector, the input data elements signs are randomly inverted with probability 1/2. The sparse transformation matrix used to complete the random projection[23] can be replaced by subsampled fourier

transform[24]. Nir Ailon and Edo Liberty define $k = O(\delta^{-4} \log(N) \log^4 n)$, where N - number of instances, n - source and k - projected dimensionality, that will preserve input vector norms by a given relative error δ [24]. The reference implementation used in this work is based on Gabriel Krummender implementation of subsampled randomized Fourier transform <https://github.com/gabobert/fast-jlt/tree/master/fjlt>. This algorithm is well suited for GPU implementation as it consists of FFT followed by element-wise operation. The last step (select random D elements) introduces irregular memory access that can not be worked around unless multiple transformations are performed in parallel. Figure 3.10 shows comparative performance of dense matrix multiplication for random projection and Fast Johnson-Lindenstrauss transform. For the selected hardware configuration the latter starts to outperform matrix multiplication starting from $N \geq 16384$. It should be noted that FLJT has lower memory requirements than $O(kn/3)$ as it does not require to store transformation matrix and thus capable of projecting higher dimensional data on the same hardware.

3.3.4 Random Projection Tree Search

The random projection tree search can be performed in the same DFS manner as the k-d tree search. We may abort the search if the query point ends in the center leaf of the large node as shown in Figure 3.9 to obtain approximate solution.

3.4 Approximate Clustering Methods

The nearest neighbours search method in high dimensional space provides little benefit over exhaustive search where an exact distance is computed to each point in the database[81][28] unless the data has low intrinsic dimensionality. The approximate methods provide means to overcome this limitation by solving the problem of finding neighbours whose distance from the query point

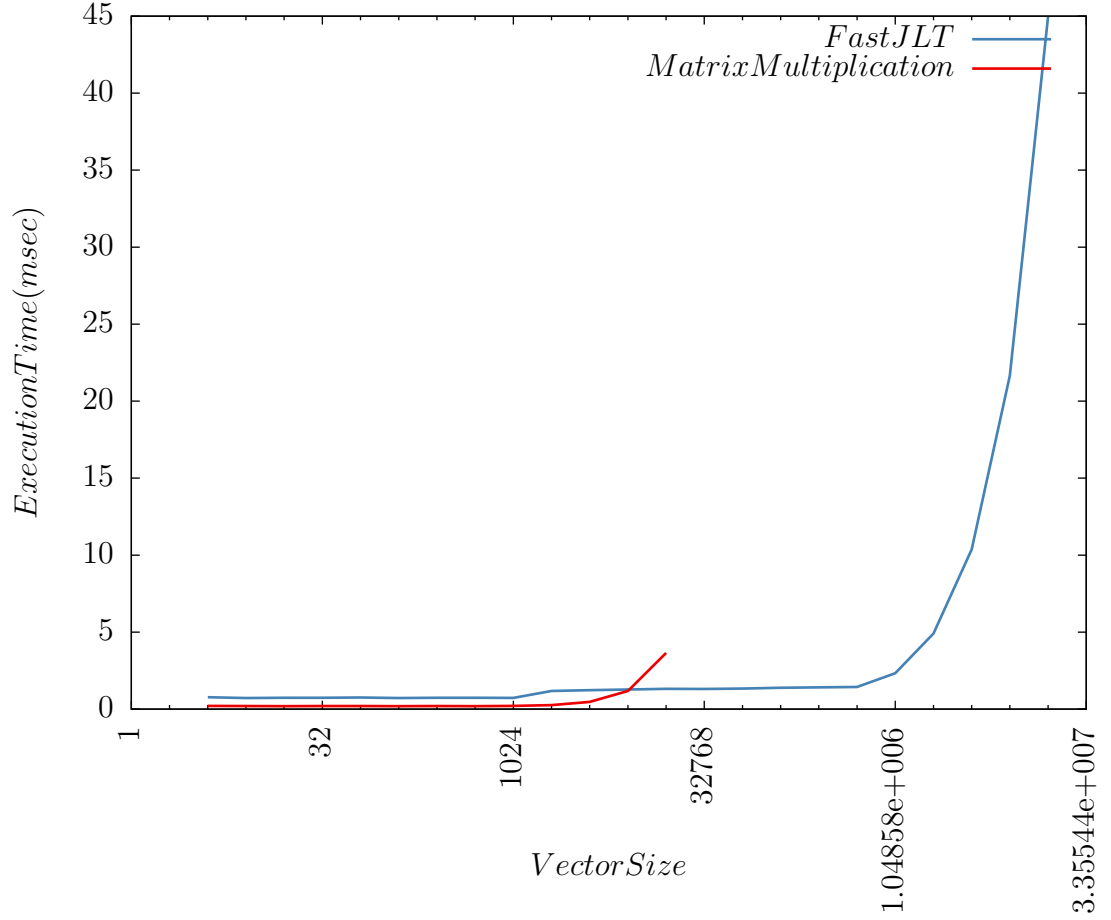


Figure 3.10: Fast Johnson-Lindenstrauss transform[24] vs. sparse matrix implementation[22] using ViennaCL. Test configuration GPU R9 390, CPU AMD A8-7600, AMD Catalyst version 15.20. The matrix multiplication test was aborted due to the out of memory error.

are at most $c > 1$ times greater than distance to the closest neighbour. The approximate solution can be used to find exact one by computing distance to each approximate nearest neighbour and choosing closest ones. Modern approximate methods use dimensionality reducing techniques such as random projection[66] and data set ordering using space filling curves[66][52][53] to improve query performance.

3.4.1 Locality Sensivity Hashing

Locality Sensivity Hashing[50] is a method that capitalizes on the idea that there exists such hash functions $h(x), x \in \mathbb{R}^d$, that for points $p, q \in \mathbb{R}^d$, radius

R and an approximation constant c the following properties hold

$$\begin{cases} \|p - q\| \leq R, P[h(p) = h(q)] \geq P_1 \\ \|p - q\| \geq cR, P[h(p) = h(q)] \leq P_2 \end{cases}$$

where probability $P_1 > P_2$. The LSH algorithm uses a concatenation of $L \ll d$ such functions to increase the difference between P_1 and P_2 [50]. Initially it was proposed to use Hamming distance as this function satisfies all required properties[50]. Later it was shown that other families of hash functions such as l_p distance[39], Jaccard coefficient [32][33] and angular distance(random projection)[35] are also locally sensitive. The algorithm selects L concatenations of the hash functions and uses them to transform input dataset points $v \in \mathbb{R}^d$ into lattice space \mathbb{Z}^L storing them as L hash tables. The exact query is performed by concatenating contents of the L bins corresponding to the hash codes of the query, and then computing exact distances. The approximation is obtained by stopping as soon as k points in cR distance from the query point are found. The method is GP GPU friendly as hash codes of the data points can be computed in massively parallel manner.

Alcantra A.F.[27] investigated several approaches to the hash table construction and retrieval on GPUs and has shown that the suitability of particular method is hardware dependent, iterative data structure content modification is difficult since insertion failure results in full hash table rebuild, which is offset by the fast rate of construction. For instance Alcantra et al[26] use tiered approach. A first-level hash function assigns an item to a bucket sized to fit into workgroup local memory and then performs rounds of cuckoo hashing[64] within the local memory until the hash table is built. Overall he notes that hash tables perform better than binary search despite uncoalesced memory access though radix sort/binary search remain a better option if queries are sorted and executed in bulk [27].

Space Filling Curves

Space filling curves[68] are curves that traverse all points of n -dimensional space in a given region providing a mapping from n -dimensional to 1-dimensional space. The GP GPU nearest neighbours algorithms[53][52][66] utilize z-order curve introduced by G. Morton in 1966 - an ordered list of numbers composed by interleaving bits of instance attributes[58]. This curve is often used due to the fact that the mapping can be constructed in $O(d)$ time and is easily implemented on GPU. A sample z-order curve is shown in Figure 3.11. A z-order

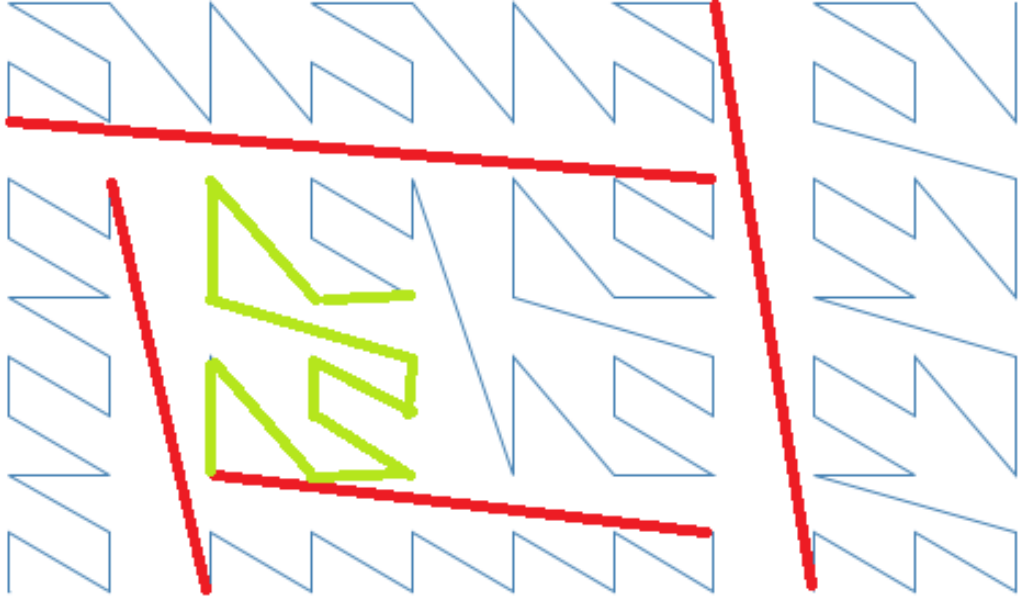


Figure 3.11: Z-Order Curve. Red lines highlight some region jumps. Green shows locality-preserving region.

curve mostly preserves data locality - points that are close in the n -dimensional space are also close together along the curve, but as shown in Figure 3.11 the z-order curve has jumps and to compensate for them existing GP GPU algorithms generate several curves from the input data shifted several times by some random vectors[53][52] to move the points into its locality-preserving regions. The shift search method by Li et al.[52] experimentally quantifies the shift value.

Sieranoja S.[73] generalized a z-order lookup table mapping algorithm for arbitrary number of dimensions. It can be translated into GPU implementa-

tion with minimal changes.

k-Nearest Neighbours using HSA architecture

The HSA architecture might allow to take OpenMP[16] approach for GP GPU acceleration of the nearest neighbours search by embedding parallel primitives such as FJLT and exhaustive search into existing algorithms without redesigning them to conform to the GPU architecture.

k-d tree queries The k-d tree queries require all or nothing approach - the algorithm design and data structures should be implemented in GP GPU specific manner to obtain higher throughput at the expense of latency[82][48]. In chapter 5 we will investigate whether it is possible to offload part of the computation to GPU without algorithm redesign to achieve performance improvement over serial version.

Random Projection Tree Construction and Queries The random projection tree tree can be built in the breadth first manner similar to existing GPU implementations of k-d tree algorithm. This approach requires pass over whole sliding window for each update. In chapter 5 we will investigate whether the online update of the random projection tree benefits from offloading projection and thresholding to GPU.

Z-Order-based queries The significant problem in z-order query evaluation is a maintenance of the candidate lists for large k [52]. The cost of GPU-host transfer in this case is prohibitive and Li et al work around it by executing multiple queries at once so that it is more beneficial to perform sort as opposed to search[52]. In chapter 5 we will investigate whether it is efficient to perform single queries using z-order lists using approach by Li et al[52] for small k .

The approximate z-order based method can utilize random projections to shorten morton code length while preserving the relative distances to speed

up queries and sliding window updates.

Conclusion Current approach to use GP GPU for k-nearest neighbours problem is to design algorithms tailored for the target GPU platform. In chapter 5 we will investigate whether it is feasible to use GPU offload in a way similar to OpenMP[16] - by replacing parts of the serial algorithm with parallel primitives. HSA platform promises smaller overhead for heterogeneous computations and in chapter 5 we will investigate whether the improvement is sufficient to disregard latency hiding methods common to the current GP GPU implementations using z-order k-nearest neighbours as an example.

Chapter 4

Stochastic Gradient Descent

4.1 Introduction

Stochastic gradient descent is an iterative optimization method used in a wide variety of machine learning tasks. It minimizes the objective function $Q(w, x)$ dependent on the set of parameters w and set of examples x by updating parameters along the gradient of the randomly chosen example x_i : $w = w - \lambda \nabla Q(w, x_i)$, where λ is the iteration step size. also called the learning rate. In classical learning applications $Q(w, x)$ is a prediction loss function and the method aims to find the set of parameters w that provides a local minimum of an error on a training set. In online learning application $Q(w, x)$ is a regret function and the method aims to provide a best approximation of $y(x)$ where y is a classification associated with example x . Stochastic gradient descent may use an average gradient of several examples - a *mini-batch* to achieve lower variance. This chapter gives an overview of the approaches for stochastic gradient descent parallelisation, describes Hogwild! and 1bit SGD algorithms used in this work, and discusses on HSA algorithm implementation.

4.2 Approaches for SGD parallelisation

The stochastic gradient descent algorithm is inherently sequential. Ways to parallelise it across computing clusters are explored in a number of papers[47][61][54][83][70].

Langford et al[83] proposed a pipelined approach to SGD parallelisation. The input vector is divided into partitions that are processed in parallel by slave worker threads producing subgradients on each step. The subgradients are sent to the master worker that recomputes the resulting parameter vector and distributes it again to the slave threads. The authors observed that algorithm sensitivity to the delay in the weights update depends on the information gained from each example and that after a certain delay threshold the algorithm performance becomes much worse [83]. This highlights a problem for any parallel implementation of SGD - one has to minimize communication to achieve maximum computation speedup without introducing critical delay that will hurt convergence of the algorithm. The subsequent works [70][47][84][41][65] provided a way to balance the parallelism and delay either by *model parallelism* - partitioning data into independent sets and processing them in parallel [47][84], delaying update communication[70][41][65], or by removing a synchronization requirement for parameters update[61]. The state of the art cluster methods use a combination of all those techniques[41][65] to solve large scale optimization problems.

The single node stochastic gradient implementation often deals with *data parallelism* - for a given mini-batch its gradients are computed in parallel. This operation requires a parallel calculation of the objective function given model parameters and a set of example instances - essentially a vector (parameters) by matrix (examples) multiplication to obtain the current approximation. Davis and Chang[40] explore single-precision matrix-vector multiplication and conclude that modern CPUs gaining last-level cache sizes and external memory bandwidth, increasing data sizes of computational problems and constrained memory size of the consumer GPU cards create a barrier to adoption of GP-GPU, though they suggest that on-chip GPUs may be excellent building blocks for future heterogeneous processors.

4.3 Hogwild!

The *Hogwild!* algorithm[61] uses an assumption that updates to the parameter vector w can be performed in a lock-free manner since each individual update only affects a small portion of it. The algorithm uses independent workers that have an access to the shared parameter vector w . Each worker samples uniformly at random an example x and computes an update vector $\lambda \nabla Q(w, x_i)$. The worker then proceeds to update each element of the parameter vector w using atomic add function. Due to multiple workers simultaneously updating the parameter vector, updates to the individual coefficients may be lost. The algorithm achieves nearly linear speedups on KDD Cup 2011[42] and Netflix prize[29] datasets [61].

4.3.1 Best Ball Optimization

The implementation of Hogwild! algorithm (<http://i.stanford.edu/hazy/victor/Hogwild/>) contains a *best ball* autotuning method. The user picks a range of model parameters (e.g. learning rate) and the algorithm evaluates the corresponding models in parallel. At the end of the epoch the model with the lowest harmonic mean of the root mean square error is selected and its parameter vector is propagated to all other models.

4.3.2 Backoff scheme

The Hogwild! algorithm uses a diminishing learning rate. The algorithm uses a global synchronization point at the end of K iterations to reduce it by a constant β and continues running for the next $\beta^{-1}K$ iterations.

4.4 1bit SGD

The Hogwild! algorithm is inherently non-deterministic. The updates of the parameter vector are performed in a lock-free manner and may be lost should

several updates contain a modification of the same parameter vector element w_i . 1Bit SGD[70] approaches the communication bottleneck from the different angle. It works on the same assumption as Hogwild! - the updates from each minibatch only affect a small portion of the parameter vector and adds a further constraint - only updates that are greater than a certain threshold should be communicated. In 1Bit SGD workers exchange gradient updates quantized to one bit - that is all workers share a quantization constant τ and communicate gradient vector element that should be updated by this constant. The difference between computed value and quantization constant is stored locally by the worker and added to the next iteration gradient update [70].

This approach allows nearly linear speed-ups in a cluster setting[78] as opposed to previous results such as[71].

4.5 Stochastic Gradient Descent using Open-CL/HSA architecture

This work implements the Hogwild! algorithm for linear models on Heterogeneous System Architecture and OpenCL platforms and compares its performance with the baseline single-threaded implementation.

The 1bit SGD thresholding is used to minimize the thread contention - only updates exceeding the quantization parameter τ are written to the shared parameter vector. This will prevent against a situation when near-zero update overwrites a bigger one.

The parameter τ is selected as per[70] - to minimize the square quantization error for a given column. The parameter is recomputed at the end of each algorithm iteration.

The algorithm is parametrized by a number of minibatches it processes simultaneously - B . The residual quantization error is stored in matrix E with each row representing the residual error for the respective mini-batch. The parallel implementation processes as follows. Sparse matrix-vector multiplica-

tion is used to obtain a vector of dot-products. For each dot product a loss function value and corresponding update value are computed. The reduce operation is used to obtain a cumulative weight update value and to average it across all minibatches. Finally a weight update kernel is launched with each thread processing separate W_{ib} - individual weight from a specific mini-batch $b \in B$. The parameter vector is updated by $\lambda\tau$, where λ - learning rate, using the atomic add function if the update value exceeds threshold, or added to corresponding element of residual error matrix E . Based on E and the iteration number an average quantization error is calculated for each column and τ used for the next iteration is updated. The pseudocode for the algorithm is presented in Figure 4.1. The 1Bit SGD technique is used to work around the lack of floating point atomic functions as the algorithm only counts number of positive and negative τ updates.

4.6 Conclusion

The proposed stochastic gradient descent algorithm is massively parallel with a single global synchronization point that occurs once in several mini-batches to recompute τ value. It can be hidden by host-GPU transfer as shown in chapter 2. Chapter 5 will compare runtimes of the algorithm on integrated and discrete GPU using HSA and OpenCL platforms respectively.

```

1  // X – input data
2  // Es,El – residual error for "too small" and "too large" cases
3  // W – weights
4  // lamda – weight update function
5  // g(x) – gradient function
6  // tau – quantization parameter vector (tau[i] > 0)
7  // temp_weights – weight updates used during training step (integer)
8  tau training_step(X, Es, El, lambda, g, tau)
9  {
10     parallel_for (mini_batch in X)
11     {
12         W = read_weights();
13         mini_batch = g(mini_batch, W); // compute gradients for each example
14         vector minibatch_gradients = average_gradients(individual_gradients) +
15         E[mini_batch];
16
17         parallel_for ( mg[i] in minibatch_gradients)
18         {
19             if (abs(mg[i]) < tau[i])
20             {
21                 // update "too small" error
22                 Es[mini_batch] = mg[i];
23             }
24             else
25             {
26                 lambda(i, sign(mg));
27                 // update "too large" error
28                 El[mini_batch] += mg < 0 ? mg[i] + tau[i] : mg[i] - tau[i];
29             }
30         }
31     }
32     commit_weights();
33     return update_tau(tau,E);
34 }
35
36 // atomic update of temporary weights
37 lambda(i, sign)
38 {
39     atomic_add(temp_weights[i],sign);
40 }
41
42 read_weights()
43 {
44     return W + learning_rate * temp_weights * tau;
45 }
46
47 commit_weights
48 {
49     W = W + learning_rate * temp_weights*tau;
50 }

```

Figure 4.1: Hogwild!-based stochastic gradient descent

Chapter 5

Experimental Results

5.1 Experiment Setup

The experiments were performed using AMD A8-7600 Radeon R7 10 Compute Cores 4C+6G CPU and integrated GPU, 16 Gb DDR3 1600 RAM and AMD Radeon R9 390 as a discrete GPU. Catalyst 15.8 drivers were used in OpenCL tests unless otherwise specified and AMDKFD driver version 1.6 was used in HSA tests unless otherwise specified. The experiments were run using Java Virtual Machine 1.8u45 for Window and Linux platforms. The operation systems used were Window 8.1 and Ubuntu Linux 14.04.

5.2 Experiment Data

The experiments used Infinimnist MNIST dataset generator[?], synthetic data streams produced by MOA[?] and Twitter data stream from January 2016. Infinimnist was used to generate a dataset containing digits from 10000 to 99999 with 783 numeric attributes and average *TODO: number* non null values. MOA data streams were used to illustrate the edge cases and validate the correctness of the algorithms implementation The twitter data was represented as a two class classification problem - two popular hashtags were chosen as classes and tweets containing them were represented as bag of words. The data generated had 5023 numeric attributes with average *TODO: number* 10

non-null values.

5.3 Evaluation

The evaluation of k-Nearest Neighbours algorithms was performed using MOA *EvaluatePeriodicHeldOutTask* with $k = 5$ unless otherwise specified.

5.4 k-Nearest Neighbours

5.4.1 Exhaustive Search

The nearest neighbours queries rely on the exhaustive search primitive to find the exact solution. The tests below used distance measures implemented as 1 instance per thread GPU kernels.

Figures 5.1, 5.2 shows latency of the algorithm and accuracy in regard to the hardware platform and precision used on Infinimnist data stream. *TODO: OpenCL Spectre, HSA spectre, float precision* The calculation precision is a limiting factor to the adoption of the more performant floating point data type on GPU. Figures 5.3, 5.4 show the accuracy of the exhaustive search on the constant size (8192) window using the synthetic MOA stream that generates a two class data stream with points uniformly distributed close to each other and different distance functions commonly used in nearest neighbour search *better wording*. The data format conversion (float-double) also incurs $O(N)$ cost on the algorithm that could be prohibitive if the cost of distance calculation is outweighed by the memory copy (or update if the operation is in-place) time as shown in Figure 5.5.

The HSA implementation shows better performance on small window sizes where discrete GPU is affected by the fixed data transfer cost and follows same performance pattern after the break-even point. The generated Twitter data stream contains extremely sparse data *TODO: average number of zeroes* and as shown in Figure 5.6 the discrete GPU transfer costs outweigh benefits until

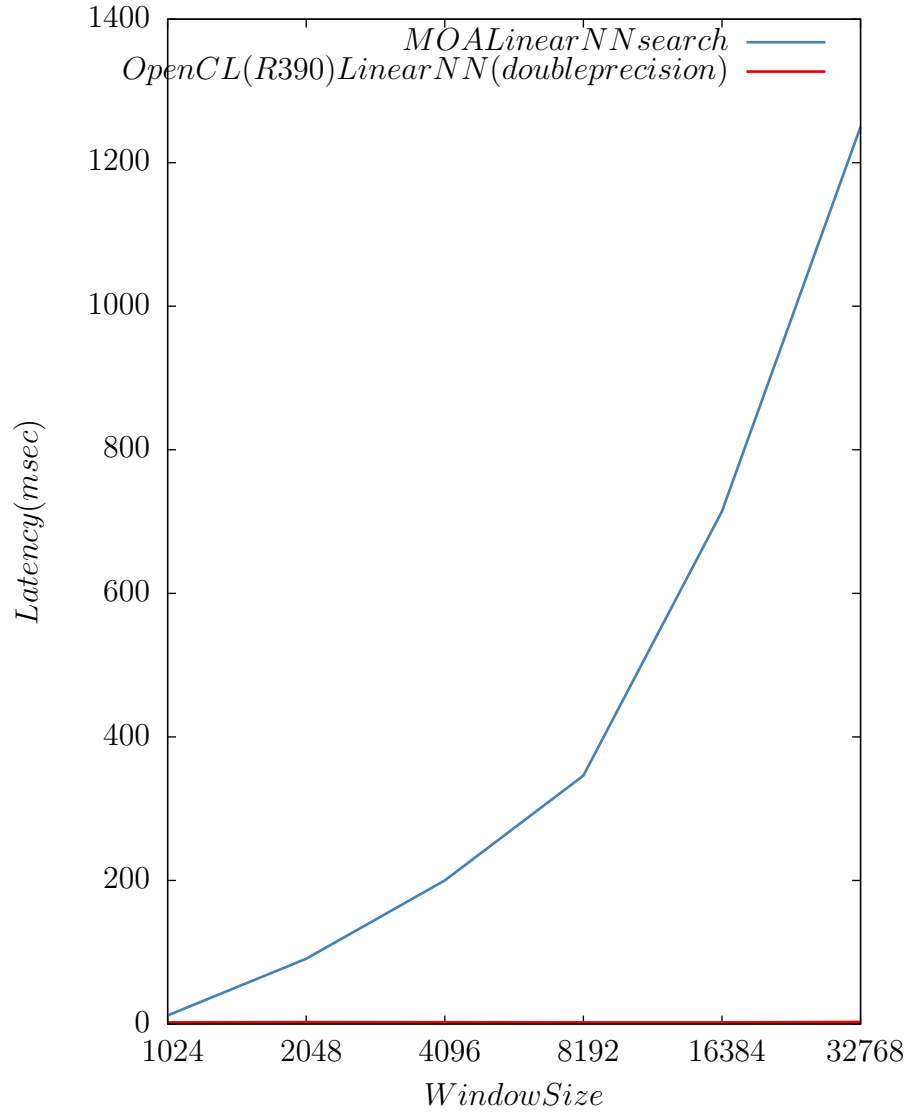


Figure 5.1: Latency of k-NN exhaustive search on Infinimnist stream

extremely large window sizes.

5.4.2 k-d Tree

It was impractical to evaluate the MOA implementation of the k-d tree performance on Infinimnist data set due to the extremely lengthy attribute min-max update procedure. The *EuclidianDistance* used by the k-d tree was replaced by the OpenCL implementation that allowed the application of k-d tree algorithm to the Infinimnist data set. In line with Figure ?? the test has shown the speed up in calculations by the discreet GPU to be outweighed by the irregular memory access patterns as shown in Figures 5.7, 5.8.

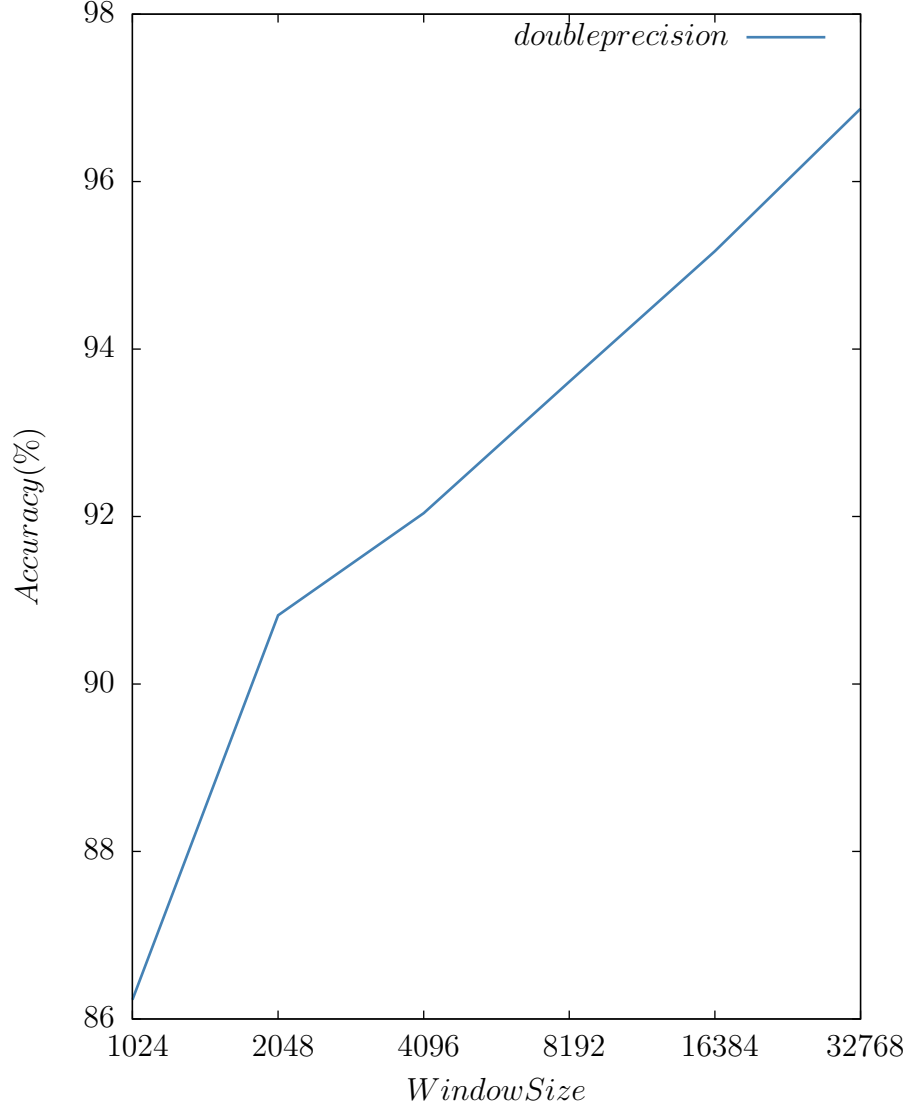


Figure 5.2: Accuracy of k-NN exhaustive search on Infinimnist stream

The high dimensionality of data provided resulted in exhaustive search outperforming k-d tree as the average number of distance calculations performed was *TODO: calculate average percent* of query size. The opposite is true for the Twitter data stream as shown in Figure 5.9. Due to the data being extremely sparse the discrete GPU offload for the query evaluation did not provide any reasonable speed up.

5.4.3 Random Projection Tree

This work uses reference serial implementation from [45] to provide a baseline benchmark of the tree performance. The projection points are computed

Figure 5.3: *TODO* Accuracy of k-NN exhaustive search on synthetic stream using constant size window (8192) and variable number of attributes

Figure 5.4: *TODO* Difference in accuracy of k-NN exhaustive search on synthetic stream using constant size window (8192) and variable number of attributes

during training phase and stored alongside the instance information incurring overhead of $(treedepth) * sizeof fp - type$ bytes. This allows to perform depth first search without recalculating the projection values during tree traversal. ‘itTODO? Spill tree hybrid? Do the defeatist search for the center split nodes? The classifier training was profiled on Infinimnist dataset with following the results: 64% of total time is spent in projection calculation, 26% in calculation of means of the attribute values. The parallelisation performed included projection calculation using either dot product or fast Johnson-Lindenstrauss transform, means update kernel and distance calculation. Figures 5.11 and ??

The average number of distance calculations per query was *TODO number*% of the window size. The random projection tree evaluation on Twitter data is presented in Figures ?? and ??.

The highest random projection tree performance speed up during training is obtained on the discrete GPU as the computationally intensive operations are offloaded in sufficient chunks and the computation does not require frequent Host-GPU synchronization. Random Projection tree query performance is higher than that of the k-d tree due to the better spatial partitioning with the average distance calculations equal to tje *todo number* 33% of the window size for Infinimnist data and *todo number* for Twitter data. The HSA implementation shows higher speed-up per GPU thread compared to discrete GPU and provides a cost-effective solution for evaluation of the nearest neighbours queries.

Figure 5.5: *TODO*Query latency of k-NN exhaustive search on synthetic stream using constant size window (8192) and variable number of attributes

Figure 5.6: *TODO*exhaustive k-NN on Twitter stream

5.4.4 Z-Order Search

The Z-Order search implementation using method proposed in [52] resulted in extremely inaccurate method when applied to Infinimnist dataset (20-40% accuracy) with a small number of curves. Adding more of them resulted in z-order search phase being prohibitively slow (more than 1 second queries). The dimensionality reduction via random projection did not alleviate the problem - the introduced distortion required even more curves to achieve more than 50% accuracy. This would not be a problem when batch approach for running queries is used as proposed in[52] as the cost of full sort for a query batch is almost the same as cost of the search for a single query[52]. The alternative implementation is iterative in regards to the search. It uses a fewer curves built on random projections of the data window and searches for nearest neighbours along the z-order curve until a stop condition such as z-order curve jump is detected. Figure 5.14 shows comparison of this method with the exhaustive search using MOA *RandomRBFGenerator* with the 1000 instances sliding window.

The change to the search phase makes the implementation exactly the same as the tree search - a chunk of data is evaluated, the stop condition checked and the process either continues or terminates. As such it shares the same characteristics with the tree search. *todo : figures*

5.5 Stochastic Gradient Descent

The Hogwild! algorithm is well-suited for the GPU implementation. It does not contain any control branches, the model updates are performed asyn-

Figure 5.7: *TODO*k-d Tree Training on Infinimnist Stream

Figure 5.8: *TODO*k-d Tree query evaluation on Infinimnist Stream

chronously and the model update data is supplied in batches. The algorithm implementation uses asynchronous transfer queue to prepare parameters for the GPU processing. The execution is pipelined and model weights are periodically copied to the output buffer to be used in prediction without explicit GPU synchronization. As such it fully benefits from the GPU architecture with the *number* speedup over serial MOA SGD implementation as shown in Figure ??.

Figure 5.9: *TODO*k-d Tree query evaluation on Twitter Stream

Figure 5.10: *TODO*Random Projection tree training on Infinimnist data

Figure 5.11: *TODO*Random Projection tree test on Infinimnist data

Figure 5.12: *TODO*Random Projection tree training on Twitter data

Figure 5.13: *TODO*Random Projection tree test on Twitter data

Figure 5.14: Iterative Z-Order query performance on RandomRBFGenerator data stream

Chapter 6

Conclusions and Future Work

6.1 HSA

The HSA platform provides means for the efficient offload of parallel computation to the GPU device where the tight coupling with the CPU is required. The traditional discrete GPUs outperform it in orders of magnitude when processing the batch tasks such as SGD classifier training but will perform on-par or slower when the algorithm requires frequent heterogeneous synchronization.

References

- [1] About openacc—www.openacc.org. http://www.openacc.org/About_OpenACC.
- [2] aparapi - api for data parallel java. allows suitable code to be executed on gpu via opencl. <https://code.google.com/p/aparapi/>.
- [3] Bolt c++ template library. <http://developer.amd.com/tools-and-sdks/opencl-zone/bolt-c-template-library>.
- [4] C++ amp overview. <https://msdn.microsoft.com/en-us/library/hh265136.aspx>.
- [5] clmath - amd. <http://developer.amd.com/tools-and-sdks/opencl-zone/amd-accelerated-parallel-processing-math-libraries/>.
- [6] Compute shader overview. <https://msdn.microsoft.com/en-us/library/windows/desktop/ff476331%28v=vs.85%29.aspx>.
- [7] cublas. <https://developer.nvidia.com/cuBLAS>.
- [8] Explaining f64 performance of gpus—arrayfire. <http://arrayfire.com/explaining-fp64-performance-on-gpus/>.
- [9] Hsafoundation. <https://github.com/HSAFoundation>.
- [10] Hsafoundation/cloc. <https://github.com/HSAFoundation/CLOC>.
- [11] Java se 7 java native interface-related apis and developer guides. <http://docs.oracle.com/javase/7/docs/technotes/guides/jni/>.
- [12] java.util.stream (java platform se 8). <http://docs.oracle.com/javase/8/docs/api/java/util/stream/package-summary.html>.
- [13] Khronos opencl registry. <https://www.khronos.org/registry/cl/>.
- [14] Nvidias next generation cuda(tm) compute architecture:fermi. http://www.nvidia.com/content/PDF/fermi_white_papers/NVIDIA_Fermi_Compute_Architecture_Whitepaper.pdf.

-
- [15] Openjdk: Project sumatra. <http://openjdk.java.net/projects/sumatra/>.
 - [16] Openmp.org. <http://openmp.org/wp/>.
 - [17] Ptx isa :: Cuda toolkit documentation. <http://docs.nvidia.com/cuda/parallel-thread-execution/index.html>.
 - [18] Renderscript—android developers. <http://developer.android.com/guide/topics/renderscript/compute.html>.
 - [19] Single instruction, multiple threads. http://en.wikipedia.org/wiki/Single_instruction,_multiple_threads#cite_note-spp-1.
 - [20] Spir - the first open standard intermediate language for parallel compute and graphics. <https://www.khronos.org/spir>.
 - [21] Hsa platform system architecture specification. <http://www.hsafoundation.com/?ddownload=4944>, 2014.
 - [22] Dimitris Achlioptas. Database-friendly random projections: Johnson-lindenstrauss with binary coins. *J. Comput. Syst. Sci.*, 66(4):671–687, June 2003.
 - [23] Nir Ailon and Bernard Chazelle. The fast johnson-lindenstrauss transform and approximate nearest neighbors. *SIAM Journal on Computing*, 39(1):302–322, 2009.
 - [24] Nir Ailon and Edo Liberty. An almost optimal unrestricted fast johnson-lindenstrauss transform. *ACM Transactions on Algorithms (TALG)*, 9(3):21, 2013.
 - [25] Tolu Alabi, Jeffrey D. Blanchard, Bradley Gordon, and Russel Steinbach. Fast k-selection algorithms for graphics processing units. *J. Exp. Algorithmics*, 17:4.2:4.1–4.2:4.29, October 2012.
 - [26] Dan A. Alcantara, Andrei Sharf, Fatemeh Abbasinejad, Shubhabrata Sengupta, Michael Mitzenmacher, John D. Owens, and Nina Amenta. Real-time parallel hashing on the gpu. In *ACM SIGGRAPH Asia 2009 Papers*, SIGGRAPH Asia '09, pages 154:1–154:9, New York, NY, USA, 2009. ACM.
 - [27] Dan Anthony Feliciano Alcantara. *Efficient hash tables on the gpu*. University of California at Davis, 2011.

-
- [28] Alexandr Andoni and Piotr Indyk. Near-optimal hashing algorithms for approximate nearest neighbor in high dimensions. *Commun. ACM*, 51(1):117–122, January 2008.
 - [29] James Bennett and Stan Lanning. The netflix prize. In *Proceedings of KDD cup and workshop*, volume 2007, page 35, 2007.
 - [30] Alina Beygelzimer, Sham Kakade, and John Langford. Cover trees for nearest neighbor. In *Proceedings of the 23rd international conference on Machine learning*, pages 97–104. ACM, 2006.
 - [31] Albert Bifet, Geoff Holmes, Richard Kirkby, and Bernhard Pfahringer. Moa: Massive online analysis. *J. Mach. Learn. Res.*, 11:1601–1604, August 2010.
 - [32] Andrei Z. Broder, Steven C. Glassman, Mark S. Manasse, and Geoffrey Zweig. Syntactic clustering of the web. In *Selected Papers from the Sixth International Conference on World Wide Web*, pages 1157–1166, Essex, UK, 1997. Elsevier Science Publishers Ltd.
 - [33] Andrei Z. Broder, Steven C. Glassman, Mark S. Manasse, and Geoffrey Zweig. Syntactic clustering of the web. *Comput. Netw. ISDN Syst.*, 29(8-13):1157–1166, September 1997.
 - [34] L. Cayton. Accelerating nearest neighbor search on manycore systems. In *Parallel Distributed Processing Symposium (IPDPS), 2012 IEEE 26th International*, pages 402–413, May 2012.
 - [35] Moses S. Charikar. Similarity estimation techniques from rounding algorithms. In *Proceedings of the Thiry-fourth Annual ACM Symposium on Theory of Computing*, STOC '02, pages 380–388, New York, NY, USA, 2002. ACM.
 - [36] T. Cover and P. Hart. Nearest neighbor pattern classification. *IEEE Trans. Inf. Theor.*, 13(1):21–27, September 2006.
 - [37] Sanjoy Dasgupta and Yoav Freund. Random projection trees and low dimensional manifolds. In *Proceedings of the Fortieth Annual ACM Symposium on Theory of Computing*, STOC '08, pages 537–546, New York, NY, USA, 2008. ACM.
 - [38] Sanjoy Dasgupta and Anupam Gupta. An elementary proof of a theorem of johnson and lindenstrauss. *Random Struct. Algorithms*, 22(1):60–65, January 2003.

- [39] Mayur Datar, Nicole Immorlica, Piotr Indyk, and Vahab S. Mirrokni. Locality-sensitive hashing scheme based on p-stable distributions. In *Proceedings of the Twentieth Annual Symposium on Computational Geometry*, SCG '04, pages 253–262, New York, NY, USA, 2004. ACM.
- [40] John D Davis and Eric S Chung. Spmv: A memory-bound application on the gpu stuck between a rock and a hard place. *Microsoft Research Silicon Valley, Technical Report14 September*, 2012, 2012.
- [41] Jeffrey Dean, Greg Corrado, Rajat Monga, Kai Chen, Matthieu Devin, Mark Mao, Andrew Senior, Paul Tucker, Ke Yang, Quoc V Le, et al. Large scale distributed deep networks. In *Advances in Neural Information Processing Systems*, pages 1223–1231, 2012.
- [42] Gideon Dror, Noam Koenigstein, Yehuda Koren, and Markus Weimer. The yahoo! music dataset and kdd-cup'11.
- [43] Peter Frankl and Hiroshi Maehara. The johnson-lindenstrauss lemma and the sphericity of some graphs. *Journal of Combinatorial Theory, Series B*, 44(3):355–362, 1988.
- [44] Yoav Freund, Sanjoy Dasgupta, Mayank Kabra, and Nakul Verma. Learning the structure of manifolds using random projections. In *Advances in Neural Information Processing Systems*, volume 20, 2007.
- [45] Yoav Freund, Sanjoy Dasgupta, Mayank Kabra, and Nakul Verma. Learning the structure of manifolds using random projections. In *Advances in Neural Information Processing Systems*, pages 473–480, 2007.
- [46] Jerome H. Friedman, Jon Louis Bentley, and Raphael Ari Finkel. An algorithm for finding best matches in logarithmic expected time. *ACM Trans. Math. Softw.*, 3(3):209–226, September 1977.
- [47] Rainer Gemulla, Erik Nijkamp, Peter J. Haas, and Yannis Sismanis. Large-scale matrix factorization with distributed stochastic gradient descent. In *Proceedings of the 17th ACM SIGKDD International Conference on Knowledge Discovery and Data Mining*, KDD '11, pages 69–77, New York, NY, USA, 2011. ACM.
- [48] Fabian Gieseke, Justin Heinermann, Cosmin Oancea, and Christian Igel. Buffer kd trees: Processing massive nearest neighbor queries on gpus. In *Proceedings of The 31st International Conference on Machine Learning*, page 172180, 2014.

- [49] Suyog Gupta, Ankur Agrawal, Kailash Gopalakrishnan, and Pritish Narayanan. Deep learning with limited numerical precision. *CoRR*, abs/1502.02551, 2015.
- [50] Piotr Indyk and Rajeev Motwani. Approximate nearest neighbors: Towards removing the curse of dimensionality. In *Proceedings of the Thirtieth Annual ACM Symposium on Theory of Computing*, STOC '98, pages 604–613, New York, NY, USA, 1998. ACM.
- [51] William Johnson and Joram Lindenstrauss. Extensions of Lipschitz mappings into a Hilbert space. In *Conference in modern analysis and probability (New Haven, Conn., 1982)*, volume 26 of *Contemporary Mathematics*, pages 189–206. American Mathematical Society, 1984.
- [52] Shengren Li, Lance Simons, Jagadeesh Bhaskar Pakaravoor, Fatemeh Abbasinejad, John D Owens, and Nina Amenta. kann on the gpu with shifted sorting. In *Proceedings of the Fourth ACM SIGGRAPH/Eurographics conference on High-Performance Graphics*, pages 39–47. Eurographics Association, 2012.
- [53] Michael D Lieberman, Jagan Sankaranarayanan, and Hanan Samet. A fast similarity join algorithm using graphics processing units. In *Data Engineering, 2008. ICDE 2008. IEEE 24th International Conference on*, pages 1111–1120. IEEE, 2008.
- [54] Dhruv Mahajan, S. Sathiya Keerthi, S. Sundararajan, and Léon Bottou. A parallel SGD method with strong convergence. *CoRR*, abs/1311.0636, 2013.
- [55] Jeremy Manson, William Pugh, and Sarita V Adve. *The Java memory model*, volume 40. ACM, 2005.
- [56] Luc Maranget, Susmit Sarkar, and Peter Sewell. A tutorial introduction to the arm and power relaxed memory models, 2012.
- [57] Duane Merrill and Andrew S. Grimshaw. High performance and scalable radix sorting: a case study of implementing dynamic parallelism for gpu computing. *Parallel Processing Letters*, 21(2):245–272, 2011.
- [58] Guy M Morton. *A computer oriented geodetic data base and a new technique in file sequencing*. International Business Machines Company New York, 1966.
- [59] Jatin Chhugani Anthony D. Nguyen Victor W. Lee Daehyun Kim Pradeep Dubey Nadathur Satish, Changkyu Kim. Fast sort on

- cpus,gpus and intel mic architectures. <http://www.intel.com/content/dam/www/public/us/en/documents/technology-briefs/intel-labs-radix-sort-mic-report.pdf>.
- [60] John Nickolls, Ian Buck, Michael Garland, and Kevin Skadron. Scalable parallel programming with cuda. *Queue*, 6(2):40–53, March 2008.
 - [61] Feng Niu, Benjamin Recht, Christopher R, and Stephen J. Wright. Hogwild: A lock-free approach to parallelizing stochastic gradient descent. In *In NIPS*, 2011.
 - [62] C. Nugteren. Improving the programmability of gpu architectures, 2014.
 - [63] Stephen Malvern Omohundro. *Five balltree construction algorithms*. International Computer Science Institute Berkeley, 1989.
 - [64] Rasmus Pagh and Flemming Friche Rodler. Cuckoo hashing. In *JOURNAL OF ALGORITHMS*, page 2004, 2001.
 - [65] Thomas Paine, Hailin Jin, Jianchao Yang, Zhe Lin, and Thomas Huang. Gpu asynchronous stochastic gradient descent to speed up neural network training. *arXiv preprint arXiv:1312.6186*, 2013.
 - [66] Jia Pan and Dinesh Manocha. Bi-level locality sensitive hashing for k-nearest neighbor computation. In *Proceedings of the 2012 IEEE 28th International Conference on Data Engineering, ICDE '12*, pages 378–389, Washington, DC, USA, 2012. IEEE Computer Society.
 - [67] P.C. Pratt-Szeliga, J.W. Fawcett, and R.D. Welch. Rootbeer: Seamlessly using gpus from java. In *High Performance Computing and Communication 2012 IEEE 9th International Conference on Embedded Software and Systems (HPCC-ICES), 2012 IEEE 14th International Conference on*, pages 375–380, June 2012.
 - [68] Hans Sagan. Space-filling curves, 1994.
 - [69] D. Sculley, Daniel Golovin, and Michael Young. Big learning with little ram. <http://citeseerx.ist.psu.edu/viewdoc/download?doi=10.1.1.298.2337&rep=rep1&type=pdf>.
 - [70] Frank Seide, Hao Fu, Jasha Droppo, Gang Li, and Dong Yu. 1-bit stochastic gradient descent and application to data-parallel distributed training of speech dnns. In *Interspeech 2014*, September 2014.
 - [71] Frank Seide, Hao Fu, Jasha Droppo, Gang Li, and Dong Yu. On parallelizability of stochastic gradient descent for speech dnns. In *Acoustics*,

- Speech and Signal Processing (ICASSP), 2014 IEEE International Conference on*, pages 235–239. IEEE, 2014.
- [72] Maxim Shevtsov, Alexei Soupikov, and Er Kapustin. Highly parallel fast kd-tree construction for interactive ray tracing of dynamic scenes.
 - [73] Sami Sieranoja. High dimensional knn-graph construction using space filling curves. <http://urn.fi/urn:nbn:fi:uef-20150325>, 2015.
 - [74] N. Sismanis, N. Pitsianis, and Xiaobai Sun. Parallel search of k-nearest neighbors with synchronous operations. In *High Performance Extreme Computing (HPEC), 2012 IEEE Conference on*, pages 1–6, Sept 2012.
 - [75] T. Aila S.Laine, T. Karras. Megakernels considered harmful: Wavefront path tracing on gpus. https://research.nvidia.com/sites/default/files/publications/laine2013hpg_paper.pdf.
 - [76] Hans Henrik Brandenborg Sørensen. High-performance matrix-vector multiplication on the gpu. In *Proceedings of the 2011 International Conference on Parallel Processing, Euro-Par’11*, pages 377–386, Berlin, Heidelberg, 2012. Springer-Verlag.
 - [77] John E Stone, David Gohara, and Guochun Shi. Opencl: A parallel programming standard for heterogeneous computing systems. *Computing in science & engineering*, 12(1-3):66–73, 2010.
 - [78] Nikko Strom. Scalable distributed dnn training using commodity gpu cloud computing. In *Sixteenth Annual Conference of the International Speech Communication Association*, 2015.
 - [79] Alan Tatourian. Nvidia gpu architecture and cuda programming environment. <http://tatourian.com/2013/09/03/nvidia-gpu-architecture-cuda-programming-environment/>.
 - [80] Philippe Tillet, Karl Rupp, Siegfried Selberherr, and Chin-Teng Lin. Towards performance-portable, scalable, and convenient linear algebra. In *Presented as part of the 5th USENIX Workshop on Hot Topics in Parallelism*, Berkeley, CA, 2013. USENIX.
 - [81] Roger Weber, Hans-Jörg Schek, and Stephen Blott. A quantitative analysis and performance study for similarity-search methods in high-dimensional spaces. In *Proceedings of the 24rd International Conference on Very Large Data Bases, VLDB ’98*, pages 194–205, San Francisco, CA, USA, 1998. Morgan Kaufmann Publishers Inc.

- [82] Kun Zhou, Qiming Hou, Rui Wang, and Baining Guo. Real-time kd-tree construction on graphics hardware. *ACM Trans. Graph.*, 27(5):126:1–126:11, December 2008.
- [83] Martin Zinkevich, John Langford, and Alex J. Smola. Slow learners are fast. In Y. Bengio, D. Schuurmans, J.D. Lafferty, C.K.I. Williams, and A. Culotta, editors, *Advances in Neural Information Processing Systems 22*, pages 2331–2339. Curran Associates, Inc., 2009.
- [84] Martin Zinkevich, Markus Weimer, Lihong Li, and Alex J Smola. Parallelized stochastic gradient descent. In *Advances in neural information processing systems*, pages 2595–2603, 2010.